

**Physiological and biochemical studies on
microbial 2'-deoxyribonucleotide biosynthesis
and oxidative pyrimidine metabolism**

Kengo Deguchi

2024

Table of Contents

General introduction	1
Chapter 1. Physiological studies on microbial 2'-deoxyribonucleotide biosynthesis	
-The design of complete synthetic medium for ribonucleotide reductase disrupted strain of <i>Escherichia coli</i> BW38029	2
Abstract	2
Introduction	2
Methods	4
Results	10
Discussion	17
Reference	19
Chapter 2. Biochemical studies on microbial oxidative pyrimidine metabolism	24
Section 1. Gene identification and enzymatic characterization of the initial enzyme in pyrimidine oxidative metabolism, uracil-thymine dehydrogenase	24
Abstract	24
Introduction	24
Methods	26
Results	29
Discussion	38
Reference	43
Section 2. Heterologous expression and characterization of ureidomalonase	45
Abstract	45
Introduction	45
Methods	48
Results	50
Discussion	55
Reference	57
Conclusion	59
Acknowledgements	61
Publications	62

General introduction

Nucleic acids (DNA and RNA) are biopolymers made of nucleotides, consisting of a base, sugar, and phosphoric acid, linked together by phosphodiester bonds. Nucleic acids play important roles in preserving, transcribing, and translating genetic information, and are essential to the central dogma, the basic principle of life. Furthermore, nucleic acids are also important substances in the industrial field. For example, trifluridine is utilized for an antiviral molecule of Herpes simplex virus (HSV), rhabdovirus, and orthopoxvirus infection. It is also utilized as an anticancer agent for metastatic colorectal cancer, and gastrointestinal tumors. Therefore, study on nucleic acid metabolism and its enzymes leads to not only the investigation of the evolution and origin of living organisms but also contributions to the industrial field.

It is speculated that nucleic acids played an important role in the early life on the primitive Earth. In the RNA world hypothesis, RNA preceded proteins and DNA, and DNA derived from RNA in primitive earth. All living organisms on the earth enzymatically synthesize deoxyribonucleotides, constituent molecules of DNA, through the process of ribonucleotide reduction, which is catalyzed by ribonucleotide reductases (RNRs). RNRs provide four deoxyribonucleoside triphosphate (dNTP) building blocks needed for DNA synthesis. The existence of RNR is one of the main grounds for the theory that DNA is derived from RNA. However, it is found that biosynthesis of deoxyribonucleosides is possible from various molecular materials by utilizing the function of enzymes in the 2-deoxyribose-5-phosphate aldolase (DERA) pathway. This indicates the possibility of existence of deoxyribonucleoside synthesis pathway that does not go through RNR. In Chapter 1, the effects of RNR gene disruption on growth of *Escherichia coli* BW38029 were investigated as a first step in verifying RNR substitution through the DERA pathway.

There are four alternative pathways for pyrimidine degradation in biological systems: the oxidative pathway, the reductive pathway, the pyrimidine utilization (rut) pathway, and the URC pathway. Of these four pyrimidine degradation pathways, the oxidative pathway is one that has not been well studied and has many unknown points. In the oxidative pathway, pyrimidine is degraded to urea and malonic acid via a barbituric acid derivative. The oxidative pathway of pyrimidine metabolism was first reported in 1952 in *Mycobacterium*, *Corynebacterium*, and *Nocardia* strains isolated from soil. However, the precise understanding of oxidative pyrimidine metabolism was not established, and only the crude extracts of microorganisms were used in these studies. Building upon these works, a study on oxidative pyrimidine metabolism in the pyrimidine-assimilating microorganism, *Rhodococcus erythropolis* JCM 3132 was initiated. This study reports on the purification and activity evaluation of uracil/thymine dehydrogenase (UTDH) (Chapter 2) and ureidomalonase (Chapter 3), which catalyze the first and third step reactions of the oxidative pathway.

Chapter 1

The design of complete synthetic medium for ribonucleotide reductase disrupted strain of *Escherichia coli* BW38029

Abstract

In all known cellular systems, synthesis of deoxyribonucleotides occurs exclusively through the process of ribonucleotide reduction, which is catalyzed by ribonucleotide reductase (RNR). Another efficient enzymatic process has been established, in which 2'-deoxyribonucleoside (dNS) is synthesized from glucose, acetaldehyde, and a nucleobase through the dNS retrosynthesis pathway. If dNSs can be synthesized in growing cells through the retrosynthesis pathway, it opens the prospect of an alternative evolutionary pathway to DNA synthesis. To confirm this hypothesis, an RNR knockout strain of *Escherichia coli* BW38029 was constructed, and its auxotrophy was investigated. This strain required only deoxycytidine among deoxyribonucleosides (dNSs) and, interestingly, nicotinamide for its growth. It was suggested that knockout of RNR may affect not only dNS synthesis but also other metabolic pathways. From these results, its complete synthetic medium was proposed, which is the MOPS medium containing dC and nicotinamide.

Introduction

All living organisms on the earth enzymatically synthesize deoxyribonucleotides, constituent molecules of DNA, through the process of ribonucleotide reduction, which is catalyzed by RNRs. RNRs provide four deoxyribonucleoside triphosphate (dNTP) building blocks needed for DNA synthesis (Jordan & Reichard, 1998; Kolberg et al., 2004; Lundin et al., 2010; Nordlund & Reichard, 2006; A. M. Poole et al., 2002). Based on the mechanism of radical formation (Jordan & Reichard, 1998; Lundin et al., 2009, 2010; A. M. Poole et al., 2002; Stubbe & van Der Donk, 1998), RNRs are grouped into three classes (Table 1-1). All three classes of RNR catalyze the cleavage of the C-OH bond at the 2' position of the ribonucleotides (A, T, G, C) and the formation of the C-H bond at the same position. The three classes of RNR share a common radical chemistry in the ribonucleotide reduction. However, they employ very different strategies for radical formation, transfer, and regeneration (Jordan & Reichard, 1998; Lundin et al., 2009, 2010; Nordlund & Reichard, 2006; A. M. Poole et al., 2002). Class I RNRs are subdivided into class Ia and class Ib. Both are composed of α 2 and β 2 dimers, and oxygen is necessary for the function. A stable tyrosyl radical is generated in the β subunit making use of the iron-oxygen center. Then the radical is transferred to the α subunit, where the reduction of the ribose (ribonucleotide) takes place. Upon reaching the active site, the radical is transferred to the ribose (ribonucleotide). Class II RNRs function under aerobic or anaerobic condition and are composed of monomer or homologous dimer (α or α 2). A 5'-deoxyadenosyl radical is generated via cleavage of deoxyadenosylcobalamin (vitamin B₁₂ coenzyme)

in class II RNRs. Unlike class I RNRs, no protein-based radical is produced in this class RNR (Jordan & Reichard, 1998; Lundin et al., 2009, 2010; Nordlund & Reichard, 2006; A. M. Poole et al., 2002). Class III RNRs function under strict anaerobic condition and are homodimers (α_2). A second protein β_2 , termed the activase (Tamarit et al., 1999), is necessary for activation of class III RNRs. The activase contains a Fe-S cluster, where a 5'-deoxyadenosyl radical is formed via cleavage of the cofactor *S*-adenosylmethionine. The produced radical is transferred to the homodimers α_2 and stored as a stable glycy radical (King & Reichard, 1995; Young et al., 1996).

In previous research about efficient enzyme synthesis of deoxyribonucleosides, it has been found that biosynthesis of deoxyribonucleosides is possible from simple molecular materials such as glucose, acetaldehyde, and nucleobase by utilizing the function of enzymes in the DERA pathway known as a reversible nucleoside degradation system (Fig. 1-1) (Horinouchi et al., 2006a; Horinouchi, Sakai, et al., 2012). In the first step of deoxyribonucleoside (dNS) degradation metabolism, purine nucleoside phosphorylase (PNP) and thymidine phosphorylase (TP) catalyze the reversible phosphorolysis of dNSs to free base and 2-deoxyribose 1-phosphate (DR1P). In the next step, phosphopentomutase (PPM) catalyzes the transfer of phosphate group between the C1 and C5 carbons of ribose to generate 2-deoxyribose 5-phosphate (DR5P). Then, DR5P is cleaved into D-glyceraldehyde 3-phosphate (G3P) and acetaldehyde; the former product is a direct intermediate in glycolysis. Therefore, dNS could be produced from glucose and acetaldehyde using reversible reactions of DERA pathway.

Retrosynthesis of dNS by the DERA pathway suggests the possibility of biosynthesis of dNS and DNA not via RNR. The possibility would raise a question about the theory that "DNA is derived from RNA" in the RNA world hypothesis (A. M. Poole, 2011; A. M. Poole et al., 2014). In this study, as a first step to verify whether dNS supply by RNR can be substituted by other pathways, the growth conditions of RNR genes-disrupted *E. coli* BW38029 were investigated to construct a synthetic medium for this strain (Table 1-2).

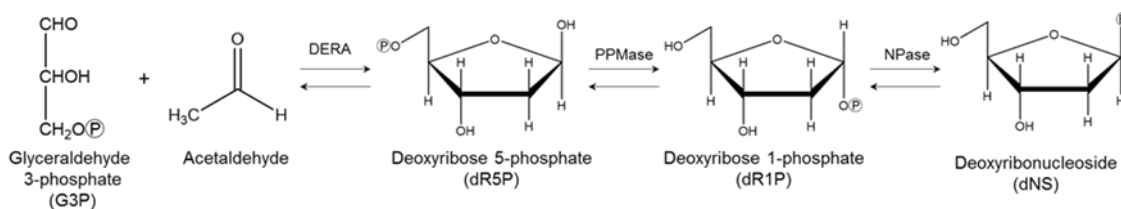


Fig. 1-1. Degradation and retrosynthesis of dNS by DERA pathway.

DERA, deoxyriboaldolase; PPMase, phosphopentomutase; NPase, nucleoside phosphorylase

Table 1-1. The classes of RNR

	ClassI	ClassII	ClassIII
Operation	Aerobic	Aerobic & anaerobic	Anaerobic
Structure	$\alpha_2\beta_2$	α or α_2	α_2 (activated by β_2)
Genes	α : <i>nrdA</i> or <i>nrdE</i> β : <i>nrdB</i> or <i>nrdF</i>	<i>nrdJ</i>	α : <i>nrdD</i> β : <i>nrdG</i>
Metal site for radical formation	Fe-O-Fe	Co (in AdoCb1)	4Fe-4S
Distribution	Eubacteria, Eukaryotes	Eubacteria, Archaea	Eubacteria, Archaea

Table 1-2. RNR in *E. coli* and the enzyme related to dNS metabolism

Gene	Enzyme	Class	Operation	Essential or not
<i>nrdA</i>	Ribonucleoside-diphosphate reductase α -subunit	Ia	Aerobic	E
<i>nrdB</i>	Ribonucleoside-diphosphate reductase β -subunit			E
<i>nrdE</i>	Ribonucleoside-diphosphate reductase α -subunit	Ib	Aerobic	E
<i>nrdF</i>	Ribonucleoside-diphosphate reductase β -subunit			E
<i>nrdD</i>	Anaerobic ribonucleoside-triphosphate reductase	III	Strict	N
<i>nrdG</i>	Anaerobic ribonucleoside reductase-activating protein		anaerobic	N

Methods

Strains and growth condition

All strains and plasmids used in this study are listed in Table 1-3. *E. coli* K-12 strain BW38029 was used as the wild-type strain for all experiments. Δ RNR, *E. coli* BW38029 Δ *nrdAB nrdEF nrdDG* with pCDF-Mmdak (Table 1-3), was grown in 5 mL LB medium (1 % (w/v) NaCl, 0.5 % (w/v) yeast extract, 1 % (w/v) tryptone with or without 2 % (w/v) agar) supplemented with 0.05 % (w/v) deoxycytidine (dC). In case of Δ RNR transformants, LB media supplemented with 0.5 % (w/v) dC, 0.17 % (w/v) yeast nitrogen base without amino acid and ammonium sulfate (YNB), and 60 nM Coenzyme B12 were used. The other strains were grown in 5 mL of LB media. Cultivation of *E. coli* was carried out at 37 °C with shaking at 300 rpm. MOPS minimal medium with 0.3 M glucose (Neidhardt et al., 1974) , and LB medium were used in growth test of Δ RNR. When necessary, 50 μ g/mL streptomycin, 50 μ g/mL kanamycin, 10 μ g/mL tetracycline, and 1 mM IPTG were added to the media.

Table 1-3. List of strains and plasmids used in this study

Strain/plasmid	Relevant genotype	Source/reference
BW38029	<i>mB3</i> ϕ (<i>lacZp4105(UV5)-lacY</i>) <i>638</i> <i>ΔlacZhsdR514 Δ(araBAD)567 rph⁺</i>	Backbone of ASKA collection, unpublished, Mori H & colleagues
ΔRNR	BW38029 <i>ΔnrnAB ΔnrnEF ΔnrnDG</i> with pCDF-Mmdak	This study
pKD46	Lambda Red recombinase expression plasmid with <i>amp^r</i> , useful in homologous recombination	(Datsenko & Wanner, 2000)
pKD-nrdAB	<i>nrdAB</i> cloned downstream of <i>exo</i> of pKD46, used in gene disruption and <i>nrdAB</i> overexpression. Ptac was inserted before the encoding region.	This study
pKD41	Containing a <i>cat-PrhaB-ccdB</i> cassette, used in amplification of <i>cat-PrhaB-ccdB</i> cassette	(Datsenko & Wanner, 2000)
pCDF-Mmdak	Gene region encoding <i>dak</i> from <i>Mycoplasma mycoides subsp.</i> <i>mycoides</i> cloned between <i>PfoI</i> and <i>XhoI</i> of pCDF; A PtacII was inserted before the encoding region	This study
pACYC-pdc	Gene region encoding <i>pdc</i> from <i>Zymomonas mobilis subsp</i> <i>mobilis</i> ATCC29191 (Brau & Sahm, 1986) cloned between <i>ScaI</i> and <i>PstI</i> of pACYC177; A PtacII was inserted before the encoding region	This study
pBR-deo	gene region encoding <i>deoC</i> , <i>deoA</i> , <i>deoB</i> , <i>deoD</i> from MG1655 inserted at the PvuI site; A PtacII was inserted before each gene	This study

pCDF-Mmdak and pKD-nrdAB construction

A pTAKN-2 vector containing sequences of the tac promoter and codon-optimized Mm-dak (pTAKN-Mmdak) was ordered to Eurofins (supplementary file). pTAKN-Mmdak and pCDF-1b (Merck, Germany) were incubated with PfoI (TAKARA BIO INC., Japan) at 37 °C for 1 hour. The plasmids treated by PfoI were purified by gel extraction utilizing FastGne Gel/PCR Extraction Kit (NIPPON Genetics, Japan). These plasmids treated by PfoI were also similarly treated with XhoI (TAKARA BIO INC., Japan). pCDF-Mmdak was constructed by ligation of these plasmids treated with PfoI and XhoI by utilizing DNA ligation kit (TAKARA BIO INC., Japan). The vector sequence was confirmed by Sanger sequencing using pCDF-PfoI-f and T7r (Table 1-4). The vector obtained was used as pCDF-Mmdak.

For construction of pKD-nrdAB, PCR was performed by Proflex PCR System (Thermo Fisher SCIENTIFIC, USA), and KOD FX (TOYOBO Corporation, Japan) was used as DNA polymerase. NrdAB-F and nrdAB-R were used as primers. The amplification conditions were 94 °C for 3 minutes, 35 cycles of 94 °C for 30 seconds, 51 °C for 30 seconds, and 72 °C for 5 minutes. The PCR product and pKD46 were incubated with SacI (TAKARA BIO INC., Japan) at 37 °C for 1 hour. pKD46-nrdAB was constructed by ligation of these fragments treated with SacI by utilizing DNA ligation kit (TAKARA BIO INC., Japan). The vector construction was confirmed by colony PCR. The vector obtained was used as pKD-nrdAB.

Table 1-4. Primers used in this study

Primer pairs		Application
Δ nrdEF1	5'-atgggtacgcaaagcgatatcgaaaacgttcgtaaagga gtaaccgaattaccggatattatcgtgagg-3'	For cloning of fragment 1-2 from pKD41, for <i>nrdEF</i> disruption
Δ nrdEF2	5'-cgggaattattccctgctgcgggtagtgatattttgaaaa taacaccaggttgaactgcggatcttg-3'	
Δ nrdEF3	5'-gaacggattcaggtagacgagccttacatc-3'	For cloning of fragment 3-6 for <i>nrdEF</i>
Δ nrdEF4	5'-tcagaaattccagctctctcgcggttgctgtgcca-3'	disruption
Δ nrdEF5	5'-ttgcaacgacaaccgacagaagactggaattctga-3'	
Δ nrdEF6	5'-tcccgtagataaggctgagagcaaatcg-3'	
Δ nrdEF7	5'-agcgtttatcgaaactgttaggtctgc-3'	For cloning of fragment 7-8 for <i>nrdEF</i>
Δ nrdEF8	5'-gcatgaattatgatcgcgcaaatcgc-3'	detection
Δ nrdDG1	5'-gccttcccaatttctgtgataacctgttcttaaaatagg agcgatcaccggatattatcgtgagg-3'	For cloning of fragment 1-2 from pKD41, for <i>nrdDG</i> disruption
Δ nrdDG2	5'-cgtaattcctcatttccctgttgcctgcactcaggtaacagg gaactaaggttgaactgcggatcttg-3'	
Δ nrdDG3	5'-catatgctgtagcggcctcatccg-3'	For cloning of fragment 3-6 for <i>nrdDG</i>
Δ nrdDG4	5'-atgacaccgatgtgatggtgcatcatttgcgatga-3'	disruption
Δ nrdDG5	5'-tcacgcaaatgatccaccatcacatcggtgcat-3'	
Δ nrdDG6	5'-ggcgcagtcgaaagacgcgtaaacg-3'	
Δ nrdDG7	5'-ccggggtttgtctgctcagatgt-3'	For cloning of fragment 7-8 for <i>nrdDG</i>
Δ nrdDG8	5'-tcggcgtcatttgcctgctgatctcg-3'	detection
Δ nrdAB1	5'-gtctgcatgaaactattcgcgaaagaattccaaaacagta cgacatacaccggatattatcgtgagg-3'	For cloning of fragment 1-2 from pKD41, for <i>nrdAB</i> disruption
Δ nrdAB2	5'-atcctggcacagcagttgtgtccagtgatcgcaggtaac gcgggccaaggttgaactgcggatcttg-3'	
Δ nrdAB3	5'-cttctgactgaactaaggtgcgcgaaagcca-3'	For cloning of fragment 3-6 for <i>nrdAB</i>
Δ nrdAB4	5'-tcagagctggaagttaactcagcagattctgattcat-3'	disruption
Δ nrdAB5	5'-atgaatcagaatctgctgagtaactccagctctga-3'	
Δ nrdAB6	5'-caggtgaaagcgtattactacgccaatgta-3'	
Δ nrdAB7	5'-gtgatgactgtgcttagatcaa-3'	For cloning of fragment 7-8 for <i>nrdAB</i>
Δ nrdAB8	5'-gcagaagctggtttctgacctgga-3'	detection
nrdAB-F	5'-aacagagctcacatacatgaatcagaatctg-3'	For cloning of fragment of <i>nrdAB</i> with SacI
nrdAB-R	5'-aacggagctcatcagagctggaagtact-3'	recognition sequence
pKD46-mut-dec3	5'-caatgctgatgacgcatcctcagc-3'	For cloning of downstream of exo of pKD46,
pKD46-mut-dec4	5'-atctcaatggtcgttctcatggc-3'	for pKD46 and pKD-nrdAB detection
pCDF-PfoI-f	5'-ggttttgcgccattcgatgg-3'	For sanger sequencing of pCDF-Mmdak
T7-r	5'-gctagtattgctcagcgg-3'	
pdC-F	5'-caggcgaattcatgattatactgctggt-3' (EcoRI)	For cloning of <i>pdC</i> from <i>Zymomonas mobilis</i> .
pdC-R	5'-ccggcaagcttctagaggagcttgaacag-3' (HindIII)	Restriction enzyme sites were underlined.
pACYC-pdC-F	5'-ccacgagtagctgagctgttgacaattaatcatcg-3' (<i>ScaI</i>)	For cloning of <i>pdC</i> from pKK-pdC.
pACYC-pdC-R	5'-atgcactgcaggtagaacgcaaaaaggcc-3' (<i>PstI</i>)	Restriction enzyme sites were underlined.

Disruption of *nrdAB*, *nrdEF*, and *nrdDG*

A two-step homologous recombination method was employed to generate *nrdEF* disruption mutant. In the first step, a 2.2 kb fragment 1-2 containing 50 bp upstream of *nrdE*, a *cat*-PrhaB-*ccdB* cassette, and 50 bp downstream of *nrdF* was amplified from pKD41 (Datsenko & Wanner, 2000), and introduced into competent cells of *E. coli* BW38029 containing pKD46 (Datsenko & Wanner, 2000). Through homologous recombination, the *nrdEF* genes of the genome were replaced by the *cat*-PrhaB-*ccdB* cassette (Fig. 1-2A). In the second step, a 700 bp fragment 3-6, composed of the upstream region of *nrdE*, the first 18 bp of *nrdE*, the last 18 bp of *nrdF*, and the downstream region of *nrdF*, was amplified by overlap extension PCR (Horton et al., 1989), and introduced into a competent mutant created in the first step. The inserted *cat*-PrhaB-*ccdB* cassette was replaced with fragment 3-6 through the second step homologous recombination (Fig. 1-2B). A scarless mutant only containing the first 18 bp of *nrdE* plus the last 18 bp of *nrdF* was constructed. The *nrdDG* was disrupted in the same method. pCDF-Mmdak cloned deoxyadenosine kinase from *Mycoplasma mycoides subsp. mycoides* was introduced in $\Delta nrdEF/\Delta nrdDG$ for support the phosphorylation of dNS. The *nrdAB* of $\Delta nrdEF/\Delta nrdDG$ with pCDF-Mmdak was disrupted using pKD-nrdAB. In order to confirm that no pKD-nrdAB remained in the obtained Δ RNR, pKD46 was introduced into the Δ RNR. Next, colony PCR was performed using Δ RNR into which pKD46 had been introduced as a template and primer pKD46-mut-dec3 and pKD46-mut-dec4. The strain, in which only a PCR product with a length unique to pKD46 was amplified, was treated as strains in which pKD46-nrdAB was removed. This strain was incubated at 37 °C on LB plate containing 0.5 % dC and pKD46 in this strain was removed because pKD46 is a temperature-sensitive plasmid. Finally, ampicillin sensitivity of this strain was confirmed by incubation of this strain on an LB plate containing 0.05 % dC and 50 μ g/mL ampicillin. The strain that showed ampicillin sensitivity was used as Δ RNR in growth test. The list of primers used in this study was shown in Table 1-4.

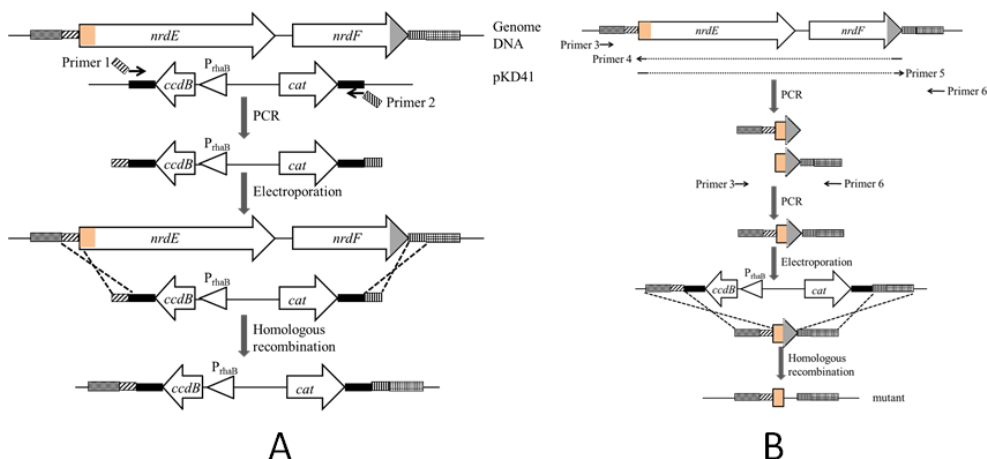


Fig. 1-2. Schematic representation of $\Delta nrdEF$ construction by overlap extension and homologous recombination.

A, fragment 1-2 cloned from pKD41 replaced *nrdEF* in the genome of *E. coli* BW38029. Strains that grew on the plate containing chloramphenicol were selected and examined, B, fragment 3-6 composed of the upstream region of *nrdE*, the first 18 bp of *nrdE* and the downstream region of *nrdF*, the last 18 bp of *nrdF*, replaced the inserted *cat-PrhaB-ccdB* cassette to form $\Delta nrdEF$. The *ccdB* is a lethal gene whose product targets DNA gyrase. Its protein is a potent cytotoxin and induces DNA strand breakage. A PrhaB, which is the rhamnose inducible promoter, located before *ccdB*, so the strain containing *cat-PrhaB-ccdB* fragment in the genome could not grow in medium containing rhamnose. The *ccdB* was used to anti-select the *nrdEF* mutant after the second recombination. Only the strains that lost the *cat-PrhaB-ccdB* could grow on a plate containing rhamnose.

Construction of *pdc* overexpression vector and *deo* operon overexpression vector.

To avoid direct supply of toxic acetaldehyde, the vector overexpressing pyruvate decarboxylase (*pdc*) was constructed. To construct the *pdc* overexpression vector, the genomic DNA of *Zymomonas mobilis* subsp. *mobilis* ATCC29191 (Brau & Sahm, 1986) was purified with DNeasy Blood & Tissue Kit (QIAGEN, USA), and the *pdc* gene was amplified with the purified genomic DNA as template, with primers *pdc*-F/R (Table 1-4). After digestion with *EcoRI* and *HindIII*, *pdc* was ligated downstream of PtacII in plasmid pKK233-3 digested with the same restriction enzymes to construct pKK-*pdc*. The PtacII-*pdc* cassette was amplified with primers pACYC-*pdc*-F/R (Table 1-4), digested with *ScaI* and *PstI*, and then ligated into pACYC177 digested with the same restriction enzymes to construct pACYC-*pdc*.

The *deo* operon, which encoded the DERA pathway enzymes, was synthesized based on the sequences of MG1655 by Biomatik (USA) and inserted into pBMH at the *PvuI* site. To express all of the four genes efficiently, PtacII and T7 terminator were inserted before and after each gene respectively. After digestion with *PvuI*, the synthesized *deo* operon was ligated into pBR322 digested with the same restriction enzyme and dephosphorylated with bacterial alkaline phosphatase (*E. coli* C75) to construct pBR-*deo*.

Colony PCR

The bacteria were cultured on an LB plate (1 % (w/v) NaCl, 0.5 % (w/v) yeast extract, 1 % (w/v) tryptone, and 2 % (w/v) agar) containing 0.5 % (w/v) dC to obtain colonies. The colonies were suspended in 8 μ L Milli Q water and incubated at 96 °C for 3 minutes. The suspension was centrifuged at 15,000 rpm for 1 minute. The supernatant (2.7 μ L) was used for the reaction, and the total volume of the reaction solution was 10 μ L. PCR was performed by Proflex PCR System (Thermo Fisher SCIENTIFIC, USA), and KOD FX (TOYOBO Corporation, Japan) was used as DNA polymerase. pKD-mut-dec3 and pKD-mut-dec4 were used as primers. The amplification conditions were 94 °C for 2 minutes and 30 cycles of 98 °C for 10 seconds, 50 °C for 30 seconds and 68 °C for 225 seconds.

The PCR product was confirmed by agarose gel electrophoresis.

***E. coli* transformation**

Transformation of *E. coli* was performed by electroporation. *E. coli* strains with knockout of all RNR genes were cultured overnight in LB media containing 0.05 % (w/v) dC. The cells were washed three times with ice-cold sterilized 10 % (v/v) glycerol and suspended in 100 μ L ice-cooled sterilized 10 % glycerol to obtain electrocompetent cells. One μ L of 10-40 (ng/ μ L) vector solution was added to 25 μ L of this electrocompetent cell. The solution was transferred to a 1 mm gap cuvette. As the vectors, pCDF-Mmdak, pKD46, pKD-nrdAB, pACYC-pdc, and pBR-deo were used. An electric pulse of 1.8 kV for 5 ms was given to it using Multiporator (Eppendorf Corporation, Germany). Immediately after applying the electric pulse, 1 mL of LB media was added to the cells and incubated at 37 °C for 1 hour. The culture was centrifuged at 10,000 rpm for 1 minute to remove 800 μ L of supernatant and then suspended. The suspension was applied to an LB plate (1 % (w/v) NaCl, 0.5 % (w/v) yeast extract, 1 % (w/v) tryptone, 2 % (w/v) agarose) containing 0.05 % or 0.5 % dC and cultured at 37 °C.

Growth test

The growth tests of Δ RNR were carried out using supplemented LB medium and MOPS minimal medium. For these tests, strains were pre-cultured in 5 mL of LB medium containing 0.05 % dC overnight, harvested by centrifugation, washed with LB medium or MOPS minimal medium, and then inoculated into 2 mL of LB medium or MOPS minimal medium at OD₆₀₀ = 0.005. These tests were carried out at 37 °C with shaking at 300 rpm. Each 0.1 % (w/v) dNS (deoxyadenosine·H₂O (dA), deoxyguanosine·H₂O (dG), deoxyinosine (dI), thymidine (dT), dC, deoxyuridine (dU)), 0.1 % (w/v) deoxyribose (dR), amino acids (0.015 % (w/v) L-tyrosine, and 0.05 % (w/v) the other 19 kinds of L-amino acids), 0.17 % (w/v) yeast nitrogen base without amino acids and ammonium sulfate (YNB), and/or vitamins (2 mg/L inositol, 0.4 mg/L nicotinamide, 0.4 mg/L pyridoxine HCl, 0.4 mg/L thiamine HCl, 0.4 mg/L calcium pantothenate, 0.2 mg/L riboflavin, 0.2 mg/L *p*-aminobenzoic acid, 2 μ g/L folic acid, 2 μ g/L biotin, and 60 nM coenzyme B12) were added when necessary. 50 μ L culture was sampled and diluted with 150 μ L MilliQ water followed by OD₆₀₀ measurement utilizing SpectraMax ABS Plus (Molecular Devices, USA). The OD₆₀₀ of three cultured media of the same composition was measured, and the average and standard error of the obtained OD₆₀₀ were calculated.

Enzymatic retrosynthesis of dNSs

E. coli transformants [Δ RNR(pBR-deo, pACYC-pdc)] were cultivated in the medium described above with 1.0 mM IPTG at 37 °C overnight. The cells were harvested by centrifugation (3,000 rpm for 10 minutes), washed with 0.85 % NaCl, and prepared for reaction. Cells were stored at

-20 °C. The reaction mixture was 200 µL and included 600 mM glucose, 250 mM sodium pyruvate, 100 mM adenine or cytosine (saturated), 24 mM MgSO₄·7H₂O, 20 mM potassium phosphate buffer (pH 7.0), 1.0 mM MnCl₂·4H₂O, 0.1 mM glucose 1,6-diphosphate, 1.0 % (v/v) xylene, and 15 % (w/v) wet cells of ΔRNR(pBR-deo, pACYC-pdc) or ΔRNR cells. The reactions were carried out at 30 °C with shaking at 120 rpm for 4 hours. The reaction mixture was mixed with ice cold methanol. After centrifuge (15,000 rpm for 10 minutes), the supernatant was used for dNS production analysis by HPLC.

HPLC analysis of nucleobase and deoxyribonucleoside

The analysis was performed by a Shimadzu LC-VP system (Shimadzu, Japan) equipped with COSMOSIL Packed column 5C₁₈-AR-II 4.6ID×150 mm (Nacalai Tesque, Japan). Eluent A (10 mM ammonium acetate buffer (pH4.5)) and eluent B (acetonitrile) were used as the mobile phases at a flow rate of 1.5 mL/min. The column oven temperature was kept at 40 °C. The gradient program was as follows: 0 % B for 0–5 min, 0–5 % B for 5–10 min, 5–60 % B for 10–17.5 min, 60 % B for 17.5–22.5 min, 60–0 % B for 22.5–25 min, 0 % B for 25–30 min. The injection volume was 10 µL. The eluted compounds were monitored with a UV detector at the absorbance of 254 nm.

Results

Construction of the ΔRNR of *E. coli* BW38029.

To investigate the replacement of RNR by supplying dNS, *nrdEF* was deleted with the method described above. As shown in Fig. 1-2, the vast majority sequence of *nrdE* and *nrdF* was deleted, only the first 18 bp of *nrdE* and the last 18 bp of *nrdF* were reserved. Other genes, *nrdDG* and *nrdAB*, were also deleted in the same method. All the disruptions of RNR gene were certified by PCR (Fig. 1-3) and sequencing. pCDF-Mmdak was introduced to Δ*nrdEF*/Δ*nrdDG* strain for the support of dNS phosphorylation, followed by disruption of *nrdAB*. Finally, knockout status was confirmed by whole genome sequencing.

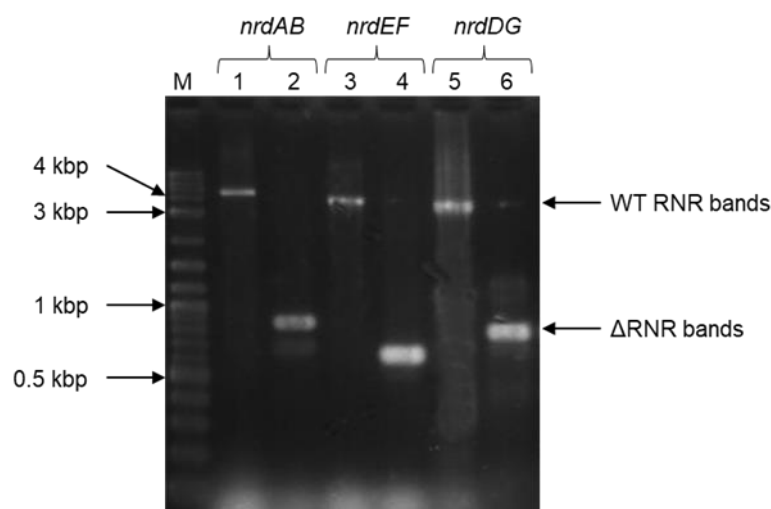


Fig. 1-3. Results of PCR with primers external to all three *nrd* operons in Δ RNR compared with the wild-type progenitor strain (BW38029).

1 kb Plus DNA Ladder was used as marker. In lanes 1, 3, and 5, the total DNA of BW38029 was used as template; in lanes 2, 4, and 6 the total DNA of the Δ RNR was used as template. In lane 1 and 2 primers for amplification of *nrdAB* were used; in lanes 3 and 4 primers for amplification of *nrdEF* were used; in lanes 5 and 6 primers for amplification of *nrdDG* were used. Lanes 1, 3, and 5, band sizes for all three operons in wild-type *E. coli* BW38029 (*nrdAB* 4471 bp, *nrdEF* 3694 bp, and *nrdDG* 3502 bp). Lanes 2, 4, and 6, band sizes consistent with operon deletion (Δ *nrdAB* 857 bp, Δ *nrdEF* 616 bp, and Δ *nrdDG* 777 bp) in the Δ RNR line.

Growth of Δ RNR in the media supplemented with dNS.

The growth of the mutant was tested and compared in the presence of dNS. The growth of Δ RNR in LB medium containing 0.02 % or 0.1 % dNS (dA, dG, dT, dC, or dU) was tested (Fig. 1-4). LB media containing 0.02 % or 0.1 % dC reached the OD₆₀₀ of 1 or 1.2, respectively, whereas Δ RNR didn't grow in the media containing other dNSs.

On the other hand, in the MOPS medium, the growth was not recovered even when dC was added (Fig. 1-5). Therefore, the medium supplemented with not only dC but also YNB, coenzyme B12 or amino acids was attempted, and the OD₆₀₀ of the media supplemented with YNB reached 0.8 to 1.4. Δ RNR did not grow in the media supplemented with only coenzyme B12 or amino acids. However, adding amino acids to the YNB-containing medium accelerated the growth. No clear effect of coenzyme B12 on the growth of Δ RNR was observed in this experiment. Next, the replacement of YNB with the vitamins contained in YNB was attempted (Fig. 1-6). Δ RNR also grew in the media that contained vitamins instead of YNB. However, the standard error of OD₆₀₀ was larger in the medium supplemented with vitamins than in the medium containing YNB. Furthermore, dNS requirement of Δ RNR was tested in MOPS media containing all the vitamins mentioned above (Fig.

1-7). Even in the MOPS medium containing the vitamins, Δ RNR strictly required dC, and OD_{600} reached 0.45. The addition of other dNSs and dR did not restore the growth of the Δ RNR strain.

In addition, the vitamin requirements of Δ RNR were also evaluated by culturing Δ RNR in MOPS media containing 9 out of the 10 types of vitamins mentioned above (Fig. 1-8) and MOPS media containing only 1 type of vitamins (Fig. 1-9). In the growth test of Fig. 1-8, OD_{600} of the medium containing all the vitamins reached 0.5. Δ RNR grew better in medium without inositol than in this medium ($OD_{600} \geq 0.7$). OD_{600} of the medium without *p*-aminobenzoic acid was comparable to that of the medium containing all the vitamins. The growth of Δ RNR was slower on media without other vitamins than on the medium with all the vitamins, and in particular, the strain did not grow on the medium without nicotinamide. When only one vitamin was added to the medium, Δ RNR grew only in the medium supplemented with nicotinamide ($OD_{600} \approx 0.14$). In the test of Fig. 1-9, OD_{600} of this medium was approximately half that of the medium supplemented with all the vitamins. From these results, it was suggested that the MOPS medium containing dC and nicotinamide was complete synthetic medium for Δ RNR.

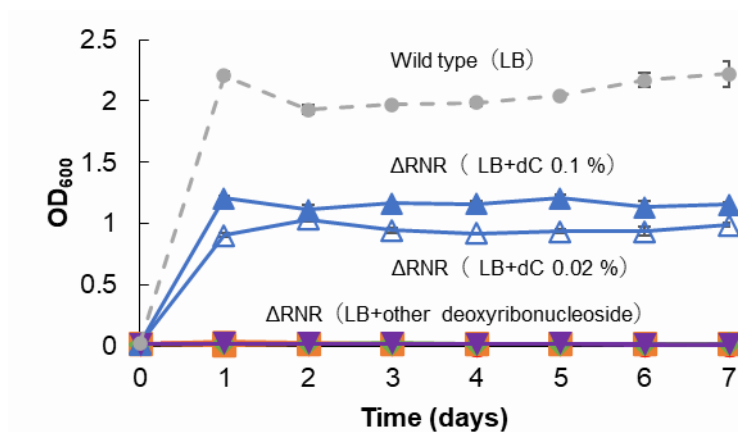


Fig. 1-4. dNS requirements of Δ RNR strains on LB medium.

Growth was monitored for Δ RNR in the media supplemented with dA (red circle), dG (orange square), dT (green rhombus), dC (blue triangle), and dU (purple inverted triangle). Closed markers indicate the media with 0.1 % (w/v) dNS concentration, and open markers indicate the media with 0.02 % (w/v) dNS concentration. Grey dashed line shows the growth curve of the wild type in LB medium.

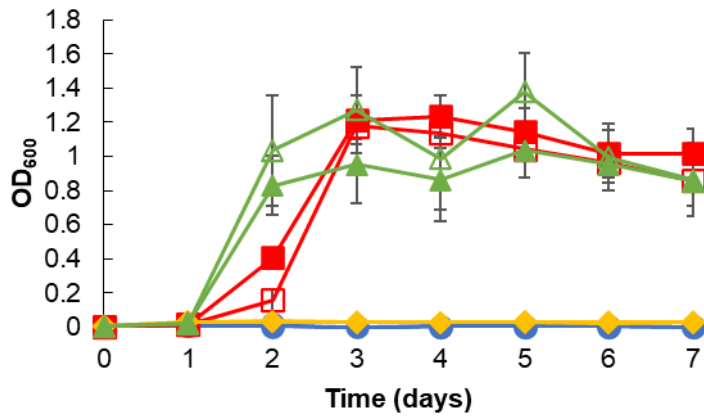


Fig. 1-5. Amino acids and vitamins requirements of Δ RNR strain in MOPS medium with 0.1 % (w/v) dC.

Blue circle shows the medium without amino acids or YNB. Red square shows the medium containing YNB. Yellow rhombus shows the medium containing amino acids. Green triangle shows the medium containing YNB and amino acids. Closed markers indicate the media with 60 nM Coenzyme B12, and open markers indicate the media without Coenzyme B12.

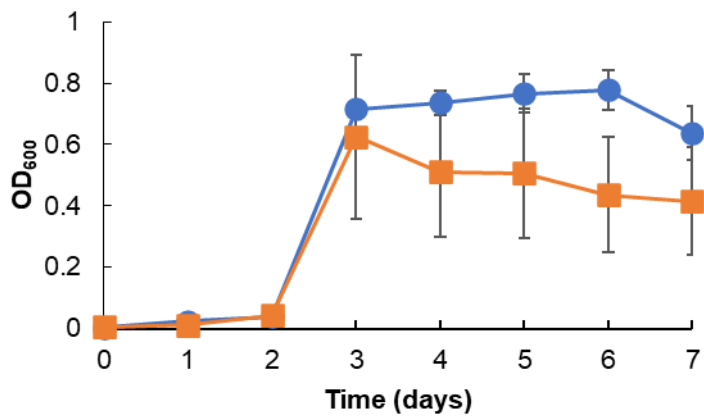


Fig. 1-6. The comparison of growth of Δ RNR in MOPS medium supplemented with YNB and medium supplemented with vitamins.

Blue circle shows the medium with YNB. Orange square shows the medium with vitamins described in Methods. Both of them contained 0.1 % (w/v) dC and 60 nM Coenzyme B12.

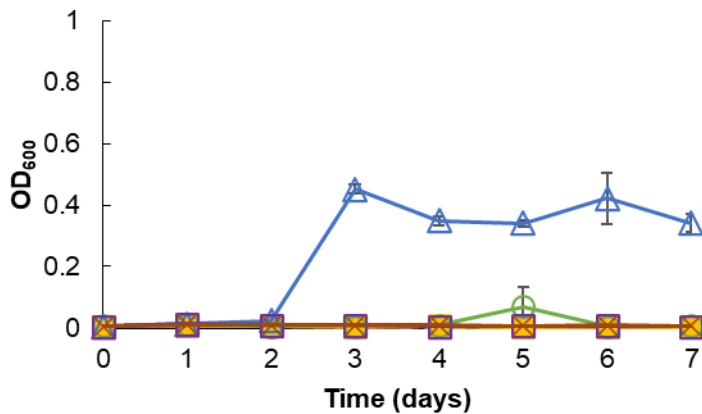


Fig. 1-7. dNS and dR requirements of Δ RNR strains in MOPS medium containing all the vitamins mentioned in methods.

Growth was monitored for Δ RNR in media supplemented with 0 % (w/v) dNS (grey cross, dash line), 0.1 % (w/v) dA (closed red circle), 0.1 % (w/v) dG (closed orange triangle), 0.1 % (w/v) dI (closed yellow square), 0.1 % (w/v) dT (open green circle), 0.1 % (w/v) dC (open blue triangle), 0.1 % (w/v) dU (open purple square), 0.1 % (w/v) dR (brown cross).

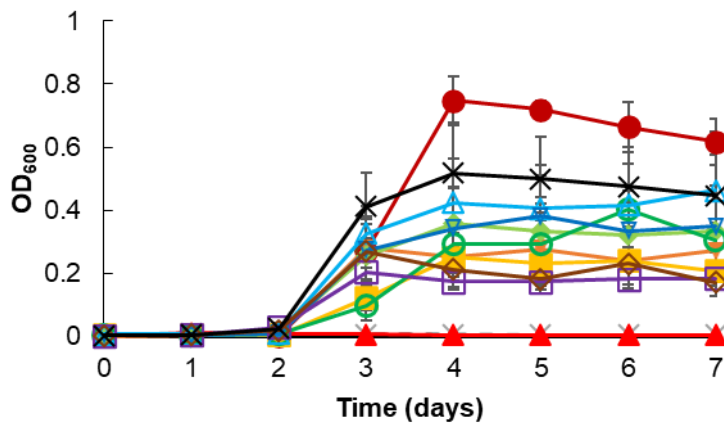


Fig. 1-8. Effects of vitamin deficiency on the growth of Δ RNR.

The author evaluated the growth of Δ RNR in MOPS medium containing 0.1 % (w/v) dC and nine vitamins other than inositol (closed dark red circle), nicotinamide (closed red triangle), pyridoxine-HCl (closed inverted triangle), thiamine-HCl (closed yellow square), calcium pantothenate (closed pale green rhombus), riboflavin (open green circle), *p*-aminobenzoic acid (open pale blue triangle), folic acid (open blue inverted triangle), biotin (open purple square), or coenzyme B12 (open brown rhombus). At the same time as culturing on these media, culturing was also performed on media with or without all vitamins (black cross or grey cross with dash line), and the growth was evaluated.

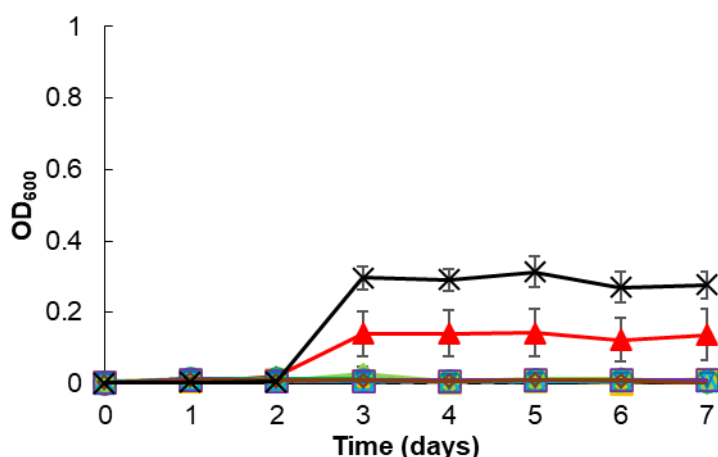


Fig. 1-9. Vitamins requirements of Δ RNR strain in MOPS medium with 0.1 % (w/v) dC.

Growth was monitored for Δ RNR in the media supplemented with inositol (closed dark red circle), nicotinamide (closed red triangle), pyridoxine-HCl (closed inverted triangle), thiamine-HCl (closed yellow square), calcium pantothenate (closed pale green rhombus), riboflavin (open green circle), p-aminobenzoic acid (open pale blue triangle), folic acid (open blue inverted triangle), biotin (open purple square), or coenzyme B12 (open brown rhombus). At the same time as culturing on these media, culturing was also performed on media with or without all vitamins (black cross or grey cross with dash line), and the growth was evaluated.

dNS production by Δ RNR overexpressing *deo* operon and *pdC*

To produce dNS via DERA pathway in Δ RNR, *deo* operon which encoded the DERA pathway enzymes was overexpressed by pBR-deo. Moreover, to avoid direct supply of toxic acetaldehyde, pyruvate decarboxylase (*pdC*) was overexpressed by pACYC-pdc. dNS production from glucose, sodium pyruvate, and adenine or cytosine by Δ RNR overexpressing *deo* operon and *pdC* was evaluated. When adenine was used, synthesis of deoxyinosine (dI), but not deoxyadenosine (dA), was confirmed (Fig. 1-10-A). Hypoxanthine, a nucleobase of dI, was also identified. When using cytosine, synthesis of deoxyuridine (dU), but not dC, was confirmed (Fig. 1-10-B). Uracil, a nucleobase of dU, was also identified.

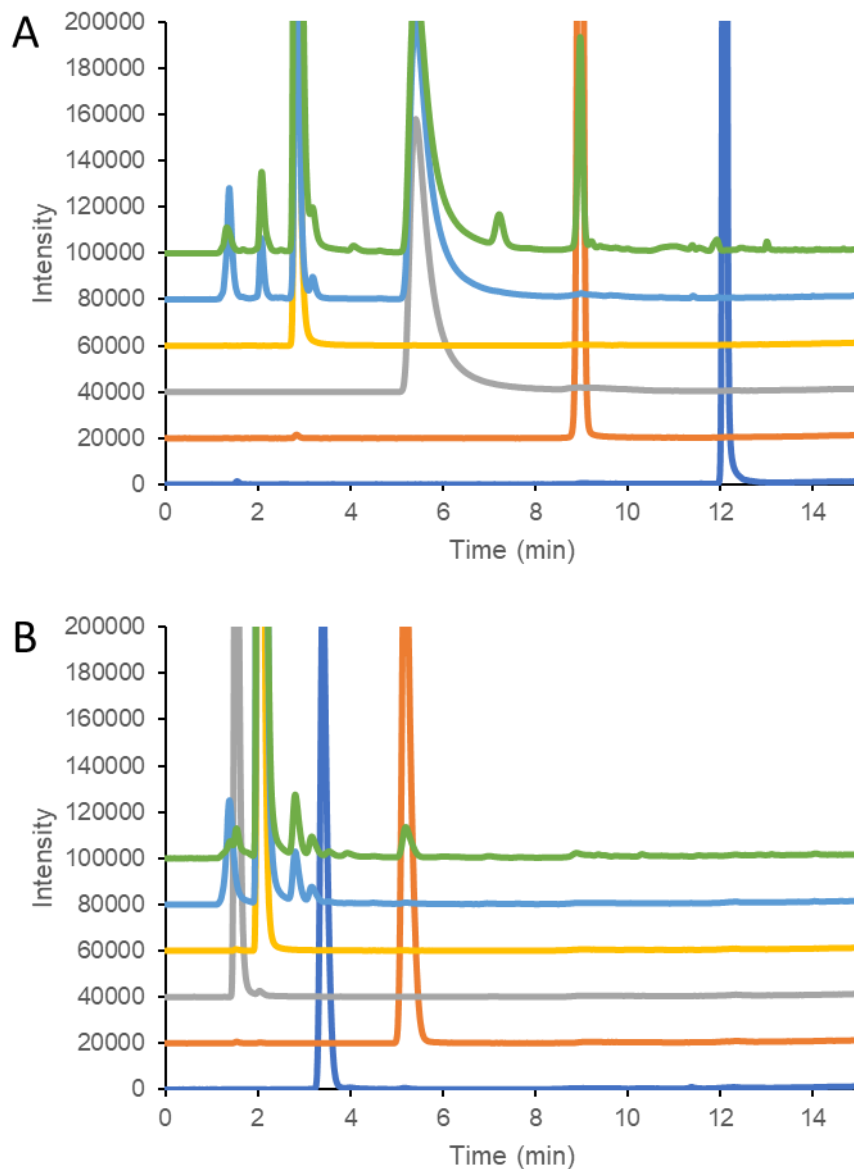


Fig. 1-10 HPLC analysis of dNS production via DERA pathway.

HPLC analysis of the reaction mixture containing 100 mM adenine (A) and cytosine (B). A: The blue chart shows 1 mM dA. The orange chart shows 1 mM dI. The grey chart shows 1 mM adenine. The yellow chart shows 1 mM hypoxanthine. The light blue chart shows the reaction mixture with ΔRNR . The green chart shows the reaction mixture with $\Delta RNR(pBR-deo, pACYC-pdc)$. B: The blue chart shows 1 mM dC. The orange chart shows 1 mM dU. The grey chart shows 1 mM cytosine. The yellow chart shows 1 mM uracil. The light blue chart shows the reaction mixture with ΔRNR . The green chart shows the reaction mixture with $\Delta RNR(pBR-deo, pACYC-pdc)$.

Discussion

At present, the RNA world hypothesis—preceding the origin of DNA and genetically encoded proteins, RNA was both genetic material and an important catalyst, and DNA originated from RNA—has become the dominant model for the biological understanding of the early evolution of life. Many observations support this hypothesis (Benner et al., 1989; Diener, 2003; Gierer & Schramm, 1956; Johnston et al., 2001; Nudler & Mironov, 2004; Talini et al., 2009), while many other observations contradict the hypothesis (Burton & Lehman, 2009; A. Poole et al., 2000; A. M. Poole & Logan, 2005; Schwarzer et al., 2003). Some reports have suggested that DNA could have a much earlier origin (Burton & Lehman, 2009; Dworkin et al., 2003; Heine et al., 2001). An efficient enzymatic process has been established in which dNSs is synthesized from glucose, acetaldehyde, and nucleobases through reverse deoxyriboaldolation (Horinouchi et al., 2006a, 2006b, 2009; Ogawa et al., 2003). This process is energy favorable and does not require multiple complex conversions. Therefore, one can easily imagine that primal organisms might favor this process for dNS synthesis at the beginning of life. The first and most important step for the verification of this hypothesis is to develop knockout strains that do not use RNR at all. In this study, a strain of *E. coli* BW38029 in which *nrdAB*, *nrdEF*, and *nrdDG* were disrupted was constructed. Then, the growth of the Δ RNR strain was evaluated in order to understand the physiological characteristics of Δ RNR strain and to construct its completely synthetic medium.

A previous study evaluated the auxotrophy of the Δ RNR strain of *E. coli* B strain Rel606 and reported that the addition of dC to the MOPS medium restored growth (Arras et al., 2023). In this study, the requirement of Δ RNR from BW38029 for not only dA, dG, dT, and dC, which were tested in our previous study, was investigated (Arras et al., 2023), but also dU, dI, and dR in MOPS medium containing vitamins (Fig. 1-7). This result indicates that only dC was used as a substrate for production of all four deoxyribonucleotides, and strongly supports the possibility shown in previous studies that dU is not a suitable substrate and deletion of *cdd*, which codes for cytidine deaminase, favors the survival of Δ RNR (Arras et al., 2023; Hosono & Kuno, 1973). On the other hand, the differences from Δ RNR strain of B strain Rel606 were observed. The Δ RNR strain of K-12 strain BW38029, like B strain Rel606, required only dC of dNS for growth, but the addition of only dC did not restore growth in MOPS medium, and vitamins were required for growth (Fig. 1-5). Even when these vitamins were added, dC was strictly required (Fig. 1-7).

In addition, the requirement for each vitamin was investigated (Fig. 1-8, 9). These results indicated that nicotinamide is essential for the growth of Δ RNR and that several other vitamins also support the growth. Nicotinamide is an intermediate in the NAD⁺ and NADP⁺ salvage pathways, and NAD⁺ can be either converted from the intermediate via this salvage pathway or synthesized *de novo* from simple amino acid precursors such as tryptophan and aspartate (Belenky, Bogan, et al., 2007; Belenky et al., 2009; Belenky, Racette, et al., 2007; Bieganowski & Brenner, 2004; Borradaile &

Pickering, 2009; Dong et al., 2014; Foster & Moat, 1980; Gerdes et al., 2006; Kurnasov et al., 2002). Therefore, it is possible that the synthesis of NAD⁺ and NADP⁺ was suppressed in Δ RNR for some reason. In addition, the presence or absence of nicotinamide auxotrophy is a major difference between the Δ RNR of the BW38029 strain in this study and the Δ RNR of Rel606 in the previous study (Arras et al., 2023). This is thought to be due to the difference in genes between the K strain and the B strain of *E. coli* or the difference in the expression level of Mm-dak. It has been confirmed that B strains such as Rel606 and K strains have genetic differences (Studier et al., 2009). Also, in the case of Δ RNR from Rel606, expression of Mm-dak was confirmed even in the absence of IPTG, but not in Δ RNR used in this study. It is possible that these differences affect vitamin requirements. However, further work is necessary to identify the reason why Δ RNR from BW38029 required not only dC but also vitamins such as nicotinamide for its growth.

A candidate alternative pathway for RNR is the deoxyribonucleoside synthesis pathway using the DERA pathway. dI and dU were synthesized by utilizing Δ RNR overexpressing *deo* operon and *pdc* (Fig. 1-10). This dNS synthesis system requires high concentrations of acetaldehyde (Horinouchi et al., 2006a; Horinouchi, Sakai, et al., 2012). However, high concentrations of acetaldehyde are toxic to living cells. Therefore, acetaldehyde was supplied from pyruvic acid by Pdc. The enzymes of this dNS synthetic pathway based on the DERA pathway were introduced into the Δ RNR using the vectors. The dNS synthesis ability of this strain that highly expresses this alternative dNS synthesis pathway was confirmed by resting bacterial cell reaction (Fig. 1-10). As a result, dI and dU were synthesized from adenine and cytosine respectively as a nucleobase of substrate via this alternative dNS synthetic pathway. This is presumed to be the result of deamination of the nucleobase used as a substrate and the generated dNS. In fact, most of cytosine in the reaction mixture is deaminated (Fig. 1-10-B). In other words, it is necessary to suppress this deamination catalyzed by cytosine/isoguanine deaminase and cytidine/deoxycytidine deaminase in order to stably supply dC necessary for the growth of Δ RNR (Hitchcock et al., 2011; Vita et al., 1985). Moreover, the catalytic activity of thymidinephosphorylase in the reaction of deoxycytidine to cytosine and deoxyribose 1-phosphate has not been confirmed (Panova et al., 2008). Therefore, there is a possibility that dC cannot be synthesized using this synthesis system. However, this problem may be solved by utilizing enzymes that synthesize dC from other dNS, such as nucleoside deoxyribosyltransferase-II (Cardinaud, 1978).

In summary, as a first step to verify whether dNS supply by RNR can be substituted by other pathways, the synthetic medium for the Δ RNR strain was determined to be MOPS medium containing dC and nicotinamide. In addition, an alternative metabolic pathway for RNR via DERA pathway was proposed as the pathway shown in Fig. 1-11.

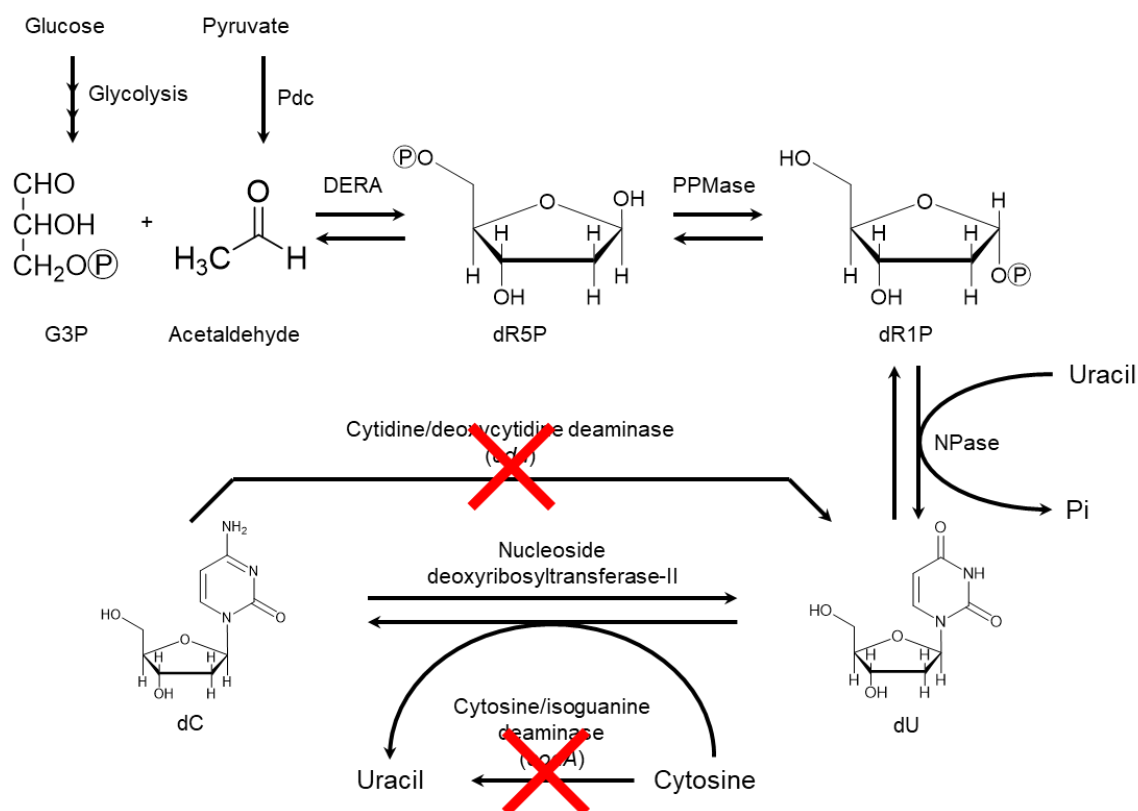


Fig. 1-11 Future plan of alternative metabolic pathway for RNR via DERA pathway.

References

- Arras, S. D. M., Sibaeva, N., Catchpole, R. J., Horinouchi, N., Si, D., Rickerby, A. M., Deguchi, K., Hibi, M., Tanaka, K., Takeuchi, M., Ogawa, J., & Poole, A. M. (2023). Characterisation of an *Escherichia coli* line that completely lacks ribonucleotide reduction yields insights into the evolution of parasitism and endosymbiosis. *eLife*, *12*. <https://doi.org/10.7554/eLife.83845>
- Belenky, P., Bogan, K. L., & Brenner, C. (2007). NAD⁺ metabolism in health and disease. *Trends in Biochemical Sciences*, *32*(1), 12–19. <https://doi.org/10.1016/j.tibs.2006.11.006>
- Belenky, P., Christensen, K. C., Gazzaniga, F., Pletnev, A. A., & Brenner, C. (2009). Nicotinamide Riboside and Nicotinic Acid Riboside Salvage in Fungi and Mammals. *Journal of Biological Chemistry*, *284*(1), 158–164. <https://doi.org/10.1074/jbc.M807976200>
- Belenky, P., Racette, F. G., Bogan, K. L., McClure, J. M., Smith, J. S., & Brenner, C. (2007). Nicotinamide Riboside Promotes Sir2 Silencing and Extends Lifespan via Nrk and Urh1/Pnp1/Meu1 Pathways to NAD⁺. *Cell*, *129*(3), 473–484. <https://doi.org/10.1016/j.cell.2007.03.024>
- Benner, S. A., Ellington, A. D., & Tauer, A. (1989). Modern metabolism as a palimpsest of the RNA world. *Proceedings of the National Academy of Sciences of the United States of America*, *86*(18), 7054–7058. <https://doi.org/10.1073/pnas.86.18.7054>

- Bieganowski, P., & Brenner, C. (2004). Discoveries of Nicotinamide Riboside as a Nutrient and Conserved NRK Genes Establish a Preiss-Handler Independent Route to NAD⁺ in Fungi and Humans. *Cell*, *117*(4), 495–502. [https://doi.org/10.1016/S0092-8674\(04\)00416-7](https://doi.org/10.1016/S0092-8674(04)00416-7)
- Borradaile, N., & Pickering, J. (2009). NAD⁺, Sirtuins, and Cardiovascular Disease. *Current Pharmaceutical Design*, *15*(1), 110–117. <https://doi.org/10.2174/138161209787185742>
- Brau, B., & Sahm, H. (1986). Cloning and expression of the structural gene for pyruvate decarboxylase of *Zymomonas mobilis* in *Escherichia coli*. *Archives of Microbiology*, *144*(3), 296–301. <https://doi.org/10.1007/BF00410966>
- Burton, A. S., & Lehman, N. (2009). DNA Before Proteins? Recent Discoveries in Nucleic Acid Catalysis Strengthen the Case. *Astrobiology*, *9*(1), 125–130. <https://doi.org/10.1089/ast.2008.0240>
- Cardinaud, R. (1978). [60] Nucleoside deoxyribosyltransferase from *Lactobacillus helveticus* (pp. 446–455). [https://doi.org/10.1016/S0076-6879\(78\)51062-8](https://doi.org/10.1016/S0076-6879(78)51062-8)
- Datsenko, K. A., & Wanner, B. L. (2000). One-step inactivation of chromosomal genes in *Escherichia coli* K-12 using PCR products. *Proceedings of the National Academy of Sciences of the United States of America*, *97*(12), 6640–6645. <https://doi.org/10.1073/pnas.120163297>
- Diener, T. O. (2003). Discovering viroids--a personal perspective. *Nature Reviews. Microbiology*, *1*(1), 75–80. <https://doi.org/10.1038/nrmicro736>
- Dong, W.-R., Sun, C.-C., Zhu, G., Hu, S.-H., Xiang, L.-X., & Shao, J.-Z. (2014). New function for *Escherichia coli* xanthosine phosphorylase (xapA): genetic and biochemical evidences on its participation in NAD⁺ salvage from nicotinamide. *BMC Microbiology*, *14*(1), 29. <https://doi.org/10.1186/1471-2180-14-29>
- Dworkin, J. P., Lazcano, A., & Miller, S. L. (2003). The roads to and from the RNA world. *Journal of Theoretical Biology*, *222*(1), 127–134. [https://doi.org/10.1016/S0022-5193\(03\)00020-1](https://doi.org/10.1016/S0022-5193(03)00020-1)
- Foster, J. W., & Moat, A. G. (1980). Nicotinamide adenine dinucleotide biosynthesis and pyridine nucleotide cycle metabolism in microbial systems. *Microbiological Reviews*, *44*(1), 83–105. <https://doi.org/10.1128/mr.44.1.83-105.1980>
- Gerdes, S. Y., Kurnasov, O. V., Shatalin, K., Polanuyer, B., Sloutsky, R., Vonstein, V., Overbeek, R., & Osterman, A. L. (2006). Comparative Genomics of NAD Biosynthesis in Cyanobacteria. *Journal of Bacteriology*, *188*(8), 3012–3023. <https://doi.org/10.1128/JB.188.8.3012-3023.2006>
- Gierer, A., & Schramm, G. (1956). Infectivity of ribonucleic acid from tobacco mosaic virus. *Nature*, *177*(4511), 702–703. <https://doi.org/10.1038/177702a0>
- Heine, A., DeSantis, G., Luz, J. G., Mitchell, M., Wong, C.-H., & Wilson, I. A. (2001). Observation of Covalent Intermediates in an Enzyme Mechanism at Atomic Resolution. *Science*, *294*(5541), 369–374. <https://doi.org/10.1126/science.1063601>
- Hitchcock, D. S., Fedorov, A. A., Fedorov, E. V., Dangott, L. J., Almo, S. C., & Raushel, F. M. (2011).

- Rescue of the Orphan Enzyme Isoguanine Deaminase. *Biochemistry*, 50(25), 5555–5557. <https://doi.org/10.1021/bi200680y>
- Horinouchi, N., Kawano, T., Sakai, T., Matsumoto, S., Sasaki, M., Mikami, Y., Ogawa, J., & Shimizu, S. (2009). Screening and characterization of a phosphopentomutase useful for enzymatic production of 2'-deoxyribonucleoside. *New Biotechnology*, 26(1–2), 75–82. <https://doi.org/10.1016/j.nbt.2009.03.015>
- Horinouchi, N., Ogawa, J., Kawano, T., Sakai, T., Saito, K., Matsumoto, S., Sasaki, M., Mikami, Y., & Shimizu, S. (2006a). Biochemical retrosynthesis of 2'-deoxyribonucleosides from glucose, acetaldehyde, and a nucleobase. *Applied Microbiology and Biotechnology*, 71(5), 615–621. <https://doi.org/10.1007/s00253-005-0205-5>
- Horinouchi, N., Ogawa, J., Kawano, T., Sakai, T., Saito, K., Matsumoto, S., Sasaki, M., Mikami, Y., & Shimizu, S. (2006b). One-pot Microbial Synthesis of 2'-deoxyribonucleoside from Glucose, Acetaldehyde, and a Nucleobase. *Biotechnology Letters*, 28(12), 877–881. <https://doi.org/10.1007/s10529-006-9019-5>
- Horinouchi, N., Sakai, T., Kawano, T., Matsumoto, S., Sasaki, M., Hibi, M., Shima, J., Shimizu, S., & Ogawa, J. (2012). Construction of microbial platform for an energy-requiring bioprocess: practical 2'-deoxyribonucleoside production involving a C-C coupling reaction with high energy substrates. *Microbial Cell Factories*, 11, 82. <https://doi.org/10.1186/1475-2859-11-82>
- Horton, R. M., Hunt, H. D., Ho, S. N., Pullen, J. K., & Pease, L. R. (1989). Engineering hybrid genes without the use of restriction enzymes: gene splicing by overlap extension. *Gene*, 77(1), 61–68. [https://doi.org/10.1016/0378-1119\(89\)90359-4](https://doi.org/10.1016/0378-1119(89)90359-4)
- Hosono, H., & Kuno, S. (1973). The Purification and Properties of Cytidine Deaminase from *Escherichia coli*. *The Journal of Biochemistry*, 74(4), 797–803. <https://doi.org/10.1093/oxfordjournals.jbchem.a130305>
- Johnston, W. K., Unrau, P. J., Lawrence, M. S., Glasner, M. E., & Bartel, D. P. (2001). RNA-catalyzed RNA polymerization: accurate and general RNA-templated primer extension. *Science (New York, N.Y.)*, 292(5520), 1319–1325. <https://doi.org/10.1126/science.1060786>
- Jordan, A., & Reichard, P. (1998). Ribonucleotide reductases. *Annual Review of Biochemistry*, 67, 71–98. <https://doi.org/10.1146/annurev.biochem.67.1.71>
- King, D. S., & Reichard, P. (1995). Mass spectrometric determination of the radical scission site in the anaerobic ribonucleotide reductase of *Escherichia coli*. *Biochemical and Biophysical Research Communications*, 206(2), 731–735. <https://doi.org/10.1006/bbrc.1995.1103>
- Kolberg, M., Strand, K. R., Graff, P., & Kristoffer Andersson, K. (2004). Structure, function, and mechanism of ribonucleotide reductases. *Biochimica et Biophysica Acta (BBA) - Proteins and Proteomics*, 1699(1–2), 1–34. <https://doi.org/10.1016/j.bbapap.2004.02.007>
- Kurnasov, O. V., Polanuyer, B. M., Ananta, S., Sloutsky, R., Tam, A., Gerdes, S. Y., & Osterman, A.

- L. (2002). Ribosylnicotinamide Kinase Domain of NadR Protein: Identification and Implications in NAD Biosynthesis. *Journal of Bacteriology*, 184(24), 6906–6917. <https://doi.org/10.1128/JB.184.24.6906-6917.2002>
- Lundin, D., Gribaldo, S., Torrents, E., Sjöberg, B.-M., & Poole, A. M. (2010). Ribonucleotide reduction - horizontal transfer of a required function spans all three domains. *BMC Evolutionary Biology*, 10, 383. <https://doi.org/10.1186/1471-2148-10-383>
- Lundin, D., Torrents, E., Poole, A. M., & Sjöberg, B.-M. (2009). RNRdb, a curated database of the universal enzyme family ribonucleotide reductase, reveals a high level of misannotation in sequences deposited to Genbank. *BMC Genomics*, 10, 589. <https://doi.org/10.1186/1471-2164-10-589>
- Neidhardt, F. C., Bloch, P. L., & Smith, D. F. (1974). Culture medium for enterobacteria. *Journal of Bacteriology*, 119(3), 736–747. <https://doi.org/10.1128/jb.119.3.736-747.1974>
- Nordlund, P., & Reichard, P. (2006). Ribonucleotide reductases. In *Annual Review of Biochemistry* (Vol. 75, pp. 681–706). <https://doi.org/10.1146/annurev.biochem.75.103004.142443>
- Nudler, E., & Mironov, A. S. (2004). The riboswitch control of bacterial metabolism. *Trends in Biochemical Sciences*, 29(1), 11–17. <https://doi.org/10.1016/j.tibs.2003.11.004>
- Ogawa, J., Saito, K., Sakai, T., Horinouchi, N., Kawano, T., Matsumoto, S., Sasaki, M., Mikami, Y., & Shimizu, S. (2003). Microbial Production of 2-Deoxyribose 5-Phosphate from Acetaldehyde and Triosephosphate for the Synthesis of 2'-Deoxyribonucleosides. *Bioscience, Biotechnology, and Biochemistry*, 67(4), 933–936. <https://doi.org/10.1271/bbb.67.933>
- Panova, N. G., Alexeev, C. S., Polyakov, K. M., Gavryushov, S. A., Kritzyn, A. M., & Mikhailov, S. N. (2008). Substrate Specificity of Thymidine Phosphorylase of *E. coli*: Role of Hydroxyl Groups. *Nucleosides, Nucleotides and Nucleic Acids*, 27(12), 1211–1214. <https://doi.org/10.1080/15257770802257895>
- Poole, A. M. (2011). On Alternative Biological Scenarios for the Evolutionary Transitions to DNA and Biological Protein Synthesis. In *Origins of Life: The Primal Self-Organization* (pp. 209–223). Springer Berlin Heidelberg. https://doi.org/10.1007/978-3-642-21625-1_10
- Poole, A. M., Horinouchi, N., Catchpole, R. J., Si, D., Hibi, M., Tanaka, K., & Ogawa, J. (2014). The case for an early biological origin of DNA. *Journal of Molecular Evolution*, 79(5–6), 204–212. <https://doi.org/10.1007/s00239-014-9656-6>
- Poole, A. M., & Logan, D. T. (2005). Modern mRNA Proofreading and Repair: Clues that the Last Universal Common Ancestor Possessed an RNA Genome? *Molecular Biology and Evolution*, 22(6), 1444–1455. <https://doi.org/10.1093/molbev/msi132>
- Poole, A. M., Logan, D. T., & Sjöberg, B.-M. (2002). The evolution of the ribonucleotide reductases: much ado about oxygen. *Journal of Molecular Evolution*, 55(2), 180–196. <https://doi.org/10.1007/s00239-002-2315-3>

- Poole, A., Penny, D., & Sjöberg, B. (2000). Methyl-RNA: an evolutionary bridge between RNA and DNA? *Chemistry & Biology*, 7(12), R207-16. [https://doi.org/10.1016/s1074-5521\(00\)00042-9](https://doi.org/10.1016/s1074-5521(00)00042-9)
- Schwarzer, D., Finking, R., & Marahiel, M. A. (2003). Nonribosomal peptides: from genes to products. *Natural Product Reports*, 20(3), 275. <https://doi.org/10.1039/b111145k>
- Stubbe, J., & van Der Donk, W. A. (1998). Protein Radicals in Enzyme Catalysis. *Chemical Reviews*, 98(2), 705–762. <https://doi.org/10.1021/cr9400875>
- Studier, F. W., Daegelen, P., Lenski, R. E., Maslov, S., & Kim, J. F. (2009). Understanding the differences between genome sequences of Escherichia coli B strains REL606 and BL21(DE3) and comparison of the E. coli B and K-12 genomes. *Journal of Molecular Biology*, 394(4), 653–680. <https://doi.org/10.1016/j.jmb.2009.09.021>
- Talini, G., Gallori, E., & Maurel, M.-C. (2009). Natural and unnatural ribozymes: back to the primordial RNA world. *Research in Microbiology*, 160(7), 457–465. <https://doi.org/10.1016/j.resmic.2009.05.005>
- Tamarit, J., Mulliez, E., Meier, C., Trautwein, A., & Fontecave, M. (1999). The anaerobic ribonucleotide reductase from Escherichia coli. The small protein is an activating enzyme containing a [4Fe-4S](2+) center. *The Journal of Biological Chemistry*, 274(44), 31291–31296. <https://doi.org/10.1074/jbc.274.44.31291>
- Vita, A., Amici, A., Cacciamani, T., Lanciotti, M., & Magni, G. (1985). Cytidine deaminase from Escherichia coli B. Purification and enzymic and molecular properties. *Biochemistry*, 24(21), 6020–6024. <https://doi.org/10.1021/bi00342a049>
- Young, P., Andersson, J., Sahlin, M., & Sjöberg, B. M. (1996). Bacteriophage T4 anaerobic ribonucleotide reductase contains a stable glycy radical at position 580. *The Journal of Biological Chemistry*, 271(34), 20770–20775. <https://doi.org/10.1074/jbc.271.34.20770>

Chapter 2

Biochemical studies on microbial oxidative pyrimidine metabolism

Section 1

Gene identification and enzymatic characterization of the initial enzyme in pyrimidine oxidative metabolism, uracil-thymine dehydrogenase

Abstract

Uracil-thymine dehydrogenase (UTDH), which catalyzes the irreversible oxidation of uracil to barbituric acid in oxidative pyrimidine metabolism, was purified from *Rhodococcus erythropolis* JCM 3132. The finding of unusual stabilizing conditions (pH 11, in the presence of NADP⁺ or NADPH) enabled the enzyme purification. The purified enzyme was a heteromer consisting of three different subunits. The enzyme catalyzed oxidation of uracil to barbituric acid with artificial electron acceptors such as methylene blue, phenazine methosulfate, benzoquinone, and α -naphthoquinone; however, NAD⁺, NADP⁺, flavin adenine dinucleotide, and flavin mononucleotide did not serve as electron acceptors. The enzyme acted not only on uracil and thymine but also on 5-halogen-substituted uracil and hydroxypyrimidine (pyrimidone), while dihydropyrimidine, which is an intermediate in reductive pyrimidine metabolism, and purine did not serve as substrates. The activity of UTDH was enhanced by cerium ions, and this activation was observed with all combinations of substrates and electron acceptors.

Introduction

Four alternative pathways for pyrimidine degradation have been reported in biological systems (Fig. 2-1): the oxidative pathway, the reductive pathway, the pyrimidine utilization (rut) pathway, and the URC pathway. In the reductive pathway, pyrimidine is degraded to β -amino acid, ammonia, and CO₂ via a dihydropyrimidine derivative (Syldatk et al., 1999; Vogels & Van der Drift, 1976) (Fig. 2-1B). The reductive pathway is widely found in mammals, plants, bacteria, and archaea. This pathway has been studied in detail because of the usefulness of dihydropyrimidinase for the synthesis of β -amino acids, as well as optically active D-amino acids, via stereoselective 5'-monosubstituted hydantoins hydrolysis by the enzyme, as well as optically active β -amino acids synthesis (Ogawa & Shimizu, 1997). Another route, the rut pathway, has been identified in *Escherichia coli* (Loh et al., 2006; Osterman, 2006; Piškur et al., 2007), in which uracil, added as a nitrogen source, is metabolized to 3-hydroxypropionic acid, ammonia, and CO₂ (Fig. 2-1C). *Lachancea kluyveri* has the URC pathway, in which uracil is converted to urea via ribosyl-urea (Andersson Rasmussen et al., 2014) (Fig. 2-1D). In the other route, the oxidative pathway, pyrimidine is degraded to urea and malonic acid via a barbituric acid derivative (Fig. 2-1A). The pyrimidine oxidative pathway was

reported in 1952 for the first time, in *Mycobacterium*, *Corynebacterium*, and *Nocardia* strains isolated from soil (Hayaishi & Kornberg, 1952; Lara, 1952). However, the precise understanding of oxidative pyrimidine metabolism was not established, and only the crude extracts of microorganisms were used in these studies. Building upon these works, a study on oxidative pyrimidine metabolism in the pyrimidine-assimilating microorganism, *Rhodococcus erythropolis* JCM 3132 was initiated (Soong et al., 2001b, 2002). The pyrimidine degrading activity of the strain had been revealed to be useful for enzymatic purine nucleoside production using nucleoside phosphorylase by controlling the reaction equilibrium by pyrimidine decomposition. Preliminary reports on the oxidative metabolism in this strain revealed that barbiturase catalyzing amide hydrolysis of barbituric acids to ureidomalonic acid and ureidomalonase, a ureidomalonic acid hydrolase, are involved in this pathway.

To date, however, there have been no studies on the physiological characteristics of uracil-thymine dehydrogenase (UTDH), which catalyzes the initial reaction of this pathway because of its unstable features. In this paper, the author report UTDH purification, identification of UTDH gene, and properties of the purified UTDH in detail.

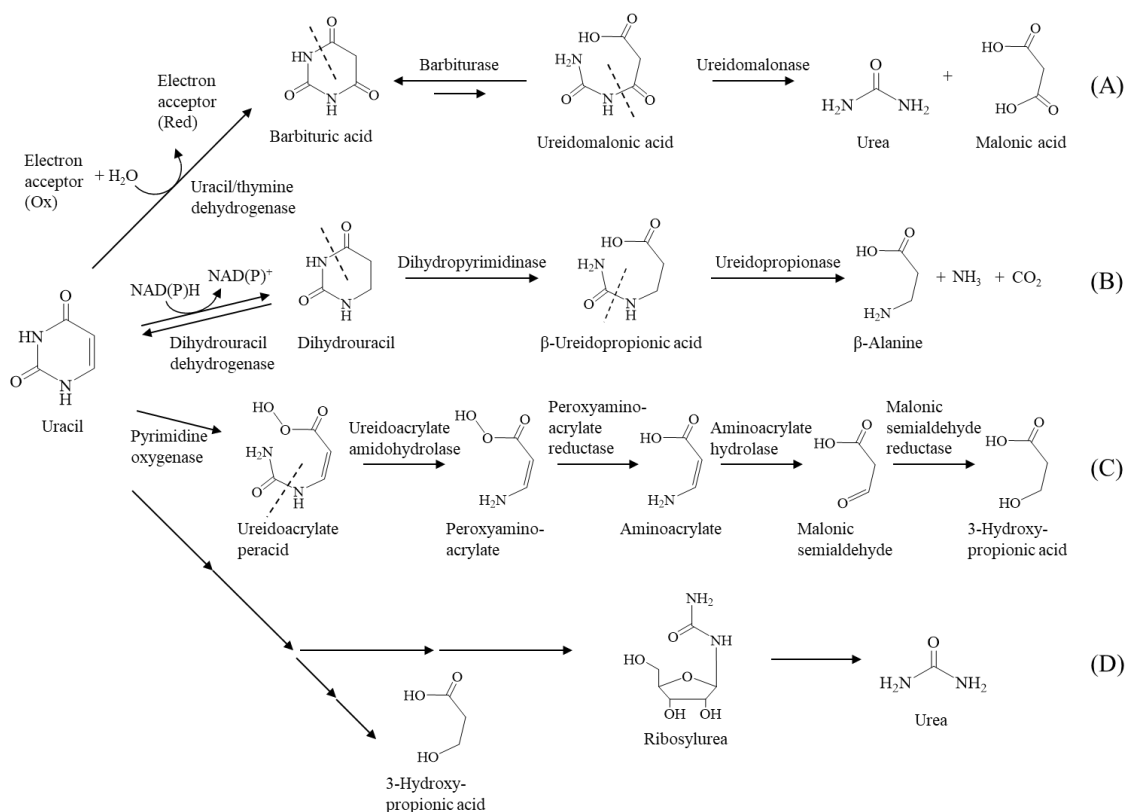


Fig. 2-1 Microbial metabolism of pyrimidine bases.

(A) Oxidative pathway (Hayaishi and Kornberg 1952; Lara 1952; Soong et al. 2001; Soong et al. 2002), (B) reductive pathway (Vogels and Drift 1976; Syldatk et al. 1999), (C) pyrimidine utilization (rut) pathway (Loh et al. 2006; Piskur et al. 2007; Osterman 2006), and (D) URC pathway (Rasmussen et

al. 2014).

Methods

Microorganisms and cultivation

Rhodococcus erythropolis JCM 3132 was cultured at 28 °C for 4 days, with shaking in uracil-rich medium (Soong et al., 2001b). In necessary, 25 µg/mL of chloramphenicol was added.

UTDH activity assay

The UTDH activity was assayed in the 100 µL reaction mixture (100 mM Tris/HCl (pH 8.5), 5 mM uracil, 1 mM methylene blue, and an aliquot of enzyme). The reaction mixtures were incubated at 30 °C for 30 min. HPLC analysis for uracil and barbituric acid was performed as described previously (Soong et al., 2001b). One unit of enzyme activity is defined as the amount of enzyme that catalyzed the consumption of substrate at the rate 1 µmol/min under the standard assay conditions.

Stability of UTDH

Frozen cells (20 % (w/v)) were suspended in various buffers (25 mM potassium phosphate, pH 7.0; 25 mM borate/NaOH, pH 10.3; 25 mM borate/NaOH, pH 11.6) with 0.5 mM NADPH or NADH at 4 °C. The cell suspensions in the above buffers were disrupted by ultrasonication at 4 °C for 20 min and then centrifuged at 14,000 × g for 60 min. The UTDH activities in the resulting supernatants of cell-free extracts (CFE) were monitored daily using standard enzyme assay conditions (described above). Optimal conditions for UTDH stability were used for purification of UTDH.

Purification of UTDH

All purification steps were carried out at 0–5 °C. The buffer used was 25 mM borate/NaOH (pH 11.6) containing 0.1 mM NADPH and 0.1 mM DTT. Washed cells (20 g) from 10 L of uracil-rich medium were harvested by centrifugation (10,000 × g at 4 °C) and suspended in 20 mL of buffer. The suspension was disrupted with 0.25- to 0.5-mm diameter glass beads (Dyno-Mill KDL, W. A. Bachofen, Switzerland) at 5 °C for 25 min. After the centrifugation (10,000 × g at 4°C), the resulting supernatant was used as the CFE. The CFEs were then injected to a DEAE-Sephacel column (2.5 × 40 cm) previously washed by 1 L of the buffer. The elution program is a linear gradient of NaCl concentration 0–1M., and the UTDH activity of fractions was confirmed in the standard condition. NaCl was added to the fractions with UTDH activity to a final concentration of 4M, and the resulting enzyme solution was injected to a phenyl-Sepharose CL-4B column (2.5 × 20 cm) washed by the buffer with 4 M NaCl. The elution program is a decreasing salt gradient (4–0 M NaCl). The active fractions were concentrated by ultrafiltration using a molecular weight 10,000 cutoff membrane. The enzyme solution was injected to a Superdex 200 HiLoad 16/600 (1.6 × 60 cm) washed by buffer

containing 0.2 M NaCl, and then eluted with the same buffer. The fractions with UTDH activity were dialyzed against 5 L of the buffer for 12 h. The resulting enzyme was applied to a MonoQ HR5/5 column (0.5 × 5 cm) previously washed by the buffer, followed by the elution of enzyme with a linear salt gradient (0–1 M NaCl). The fractions with UTDH activity were applied to a Superose-6 column (0.1 × 30 cm) previously washed by the buffer with 0.2 M NaCl. The enzyme was eluted with the same buffer, and the fractions with UTDH activity were utilized for characterization.

Protein and gene analyses

Protein concentration measurement, molecular mass analysis of proteins by gel-permeation high-performance liquid chromatography, SDS-PAGE, preparation of internal peptides for sequencing, amino acid sequencing determination of NH₂-terminal and internal amino acid sequences, and DNA manipulation and sequencing were performed as described previously (Soong et al., 2002).

Cofactor analysis

The purified UTDH (150 mg/mL) was dialyzed against 25 mM Tris/HCl (pH 7.5). The absorption spectrum of the dialyzed enzyme was measured with a microplate reader (Spectra Max 190, Molecular Devices). Fifty μL of UTDH was precipitated with 10 μL of 15 % (v/v) perchloric acid, followed by neutralization with 10 μL of 1 M potassium phosphate (pH 7.0). The supernatant was subjected to flavin analysis by HPLC (Shimadzu, Japan) equipped with an ion-exchange (QAE-2SW TSK-gel, 4.6 × 250 mm, Tosoh, Japan) eluted with 150 mM KH₂PO₄ (pH 2.5) at a flow rate of 1.0 mL/min at 40 °C. The cofactors were identified and quantified based on the retention times and peak area of the standard compounds, i.e., FAD (13.5 min), flavin mononucleotide (FMN, 10.3 min), and riboflavin (4.4 min).

PCR and inverse PCR

Two primers (5'-tggga(t/c)ggnga(t/c)ga(a/g)aa(t/c)acnttnacntt(t/c)tg-3', and 5'-(a/g)aangcngt(t/c)tg(a/g)tgnc(t/c)tgnc(t/c)tg-3', where n = any base) were produced based on two internal peptide sequences, WGDENTLTFW and QGQGHQTAF, respectively. PCR was performed as described previously (Soong et al., 2002), except that primers and PCR cycles. Above primers and Thermoblock T-Gradient (Biometra, Germany) was used for PCR. The PCR conditions were 94 °C for 5 minutes, 30 cycles of 94 °C for 1 minute, 60 °C for 2 minutes and 72 °C for 3 minutes, and 72 °C for 5 minutes. The 900 bp PCR product was ligated into a TA cloning vector pCR2.1 (Invitrogen), yielding pCR-UTDH1. The electroporation was performed by a Bio-Rad Gene-Pulser for the transformation into *E. coli* JM109. Screening for positive transformants was performed by *EcoRI* treatment of purified plasmid. The 900-bp insert was confirmed by sequencing with M13 forward and reverse primers.

The inverse PCR was performed for the cloning of the upstream and downstream regions flanking the inserted gene. The genomic DNA was separately treated with several restriction enzymes, the restriction sites of which did not exist in the cloned 900-bp gene. A *Bam*HI digest of 4.6-kbp was selected by Southern blot analysis. One µg/mL of genomic DNA was then treated with *Bam*HI followed by self-ligation. PCR of this ligated DNA was performed utilizing two primers (S1, 5'-agaagctcatcgactgggacggatt-3', and AS1, 5'-gggtgaacgatcttgacgccgaatccac-3'). The 4.6-kb PCR product was purified, ligated into a TA cloning vector, followed by the transformation into *E. coli* JM109. The screening for positive colonies was performed by colony hybridization. The resulting cloned plasmid, pCR-UTDH2, was isolated and sequenced.

Construction of UTDH overexpression strain

The UTDH gene (Accession number: AB250759.1) was amplified by PCR using the following primers: 5'-TGTTTAACTTTAAGAAGGAGATATAACCATGAAACCGTCGCCGCTGAC-3' and 5'-TGGTGATGGTGTGCTCGAGAGATCTATCATGCATTCTCCTCTGATG-3'. PrimeSTAR Max DNA polymerase (Takara, Shiga, Japan) was utilized for PCR. The PCR conditions were 94 °C for 1 minutes, and 30 cycles of 98 °C for 10 seconds, 69 °C for 5 seconds, and 72 °C for 20 seconds. pTipQC1 (Hokkaido System Science, Hokkaido, Japan) was treated with *Hind*III and *Nco*I, followed by the purification by gel electrophoresis. The digested product combined with the PCR products utilizing NEBuilder HiFi DNA Assembly (New England Biolabs, Massachusetts, USA). The resulting plasmid, pTipQC1/UTDH, was transformed into *Rhodococcus erythropolis* L88 (Hokkaido System Science, Hokkaido, Japan).

Homologous expression of recombinant UTDH

The *Rhodococcus erythropolis* pTipQC1/UTDH was cultivated in 5 mL of pre-culture LB medium at 28 °C with shaking at 300 rpm for overnight. The resulting pre-culture was inoculated into 90 mL of LB medium with 0.2 mg/L of FeSO₄·7H₂O, Na₂MoO₄·2H₂O, MnSO₄·nH₂O, CuSO₄·5H₂O, and ZnCl₂. The main culture was incubated at 28 °C with shaking at 120 rpm for 3 h, followed by the addition of 0.2 µg/mL of thiostrepton to the main culture. After the addition of thiostrepton, the culture was incubated at 28 °C with shaking at 120 rpm for 1 day. The transformed cells were harvested from 200 mL of culture and suspended in 20 mmol/L potassium phosphate pH 8.0 at twice volume of the cell weight. The cell suspension (400 µl) and 0.4 g of 0.1 mm low-alkaline glass beads were mixed in tube and treated with Multi-beads shocker (Yasui Kikai, Osaka, Japan) under the following conditions: temperature, 0 °C; speeds of rotation, 2,500 rpm; time program, ON TIME 60 s, OFF TIME 60 s, 6 cycles. The cell debris was removed by centrifugation at 1,700 g for 15 min. The resulting supernatant was used as the CFE.

CFE reaction was carried out at 30 °C with shaking at 1000 rpm for 2 h. The reaction mixture contained 5 mM uracil, 1 mM methylene blue, and 10 % (v/v) of CFE in 20 mmol/L potassium phosphate pH 8.0.

Results

Stabilization of UTDH activity in the CFE

Unstable feature of UTDH activity in the CFE made impossible its purification. For UTDH purification, various conditions were examined to retain the enzyme activity (pH and coexistence of cofactors and substrates). UTDH activity completely disappeared after 4 days when the CFE were kept in 25 mM potassium phosphate buffer (pH 7.0) at 4 °C. UTDH activity was stable at unusual alkaline conditions, over pH 10.5, with the presence of NADP⁺ or NADPH (Fig. 2-2). Enzyme purification was carried out in 25 mM borate/NaOH (pH 11.6), in the presence of NADPH.

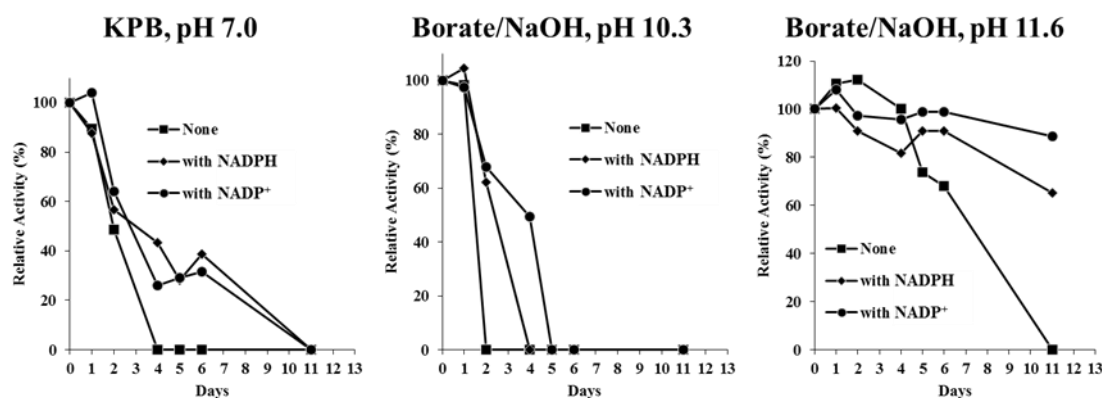


Fig. 2-2 Effects of pH and NADPH/NADP⁺ on the stability of UTDH.

Frozen cells (20 %, w/v) were suspended in each 25 mM buffer without or with the presence of 0.5 mM NADPH or NADP⁺. The cell suspension was then subjected to sonication, and cell-free extracts were obtained after centrifugation. UTDH activity in the cell-free extracts was monitored daily.

Electron acceptors

The effects of electron acceptors on uracil oxidation to barbiturate by UTDH were examined using cell-free extracts of *R. erythropolis* JCM 3132 as the enzyme source under standard enzyme assay conditions. It was found that methylene blue, phenazine methosulfate, benzoquinone, α -naphthoquinone, and dichlorophenolindophenol served as electron acceptors, whereas FAD, flavin mononucleotide (FMN), NAD⁺, and NADP⁺ did not (Table 2-1). Further analysis was conducted with methylene blue as a standard electron acceptor.

Table 2-1 Effect of electron acceptors

Electron acceptors	Relative activity (%)
Methylene blue	100
Phenazine methosulfate	79
Benzoquinone	31
α -Naphthoquinone	41
Dichlorophenolindophenol	12
FAD	1
FMN	5
NAD ⁺	0
NADP ⁺	1
None	5

Reactions were performed using standard enzyme assay conditions (described in Methods) with each electron acceptor (1 mM).

Purification, molecular weight, and cofactor contents

Using 25 mM borate/NaOH (pH 11.6) containing 0.1 mM NADPH and 0.1 mM DTT as a purification buffer, UTDH was purified by column chromatography with activity detection by barbituric acid generation from uracil with methylene blue as an electron acceptor. The overall yield of purified UTDH was 10 % and the specific activity was increased by 320-fold (Table 2-2). When analyzed by gel-permeation high-performance liquid chromatography (HPLC) using a G3000SW column, a symmetrical peak of purified enzyme was observed. In comparison with marker proteins, the relative molecular mass of the native enzyme was estimated to be over 290,000. Analysis of the purified enzyme by SDS-PAGE revealed three different protein bands with relative molecular mass of 90,000 (large subunit; L-subunit), 35,000 (medium subunit; M-subunit), and 25,000 (small subunit; S-subunit) (Fig. 2-3A). These results indicated that the native enzyme consists of three different subunits.

It was expected that this enzyme contained flavin because the absorption spectrum of the purified enzyme showed maximum absorbance at 440 nm (Fig 2-3B). The centrifuged supernatant of the enzyme solution treated with perchloric acid was analyzed by HPLC. The results revealed that this enzyme contained 1.7 moles of FAD per mole of protein.

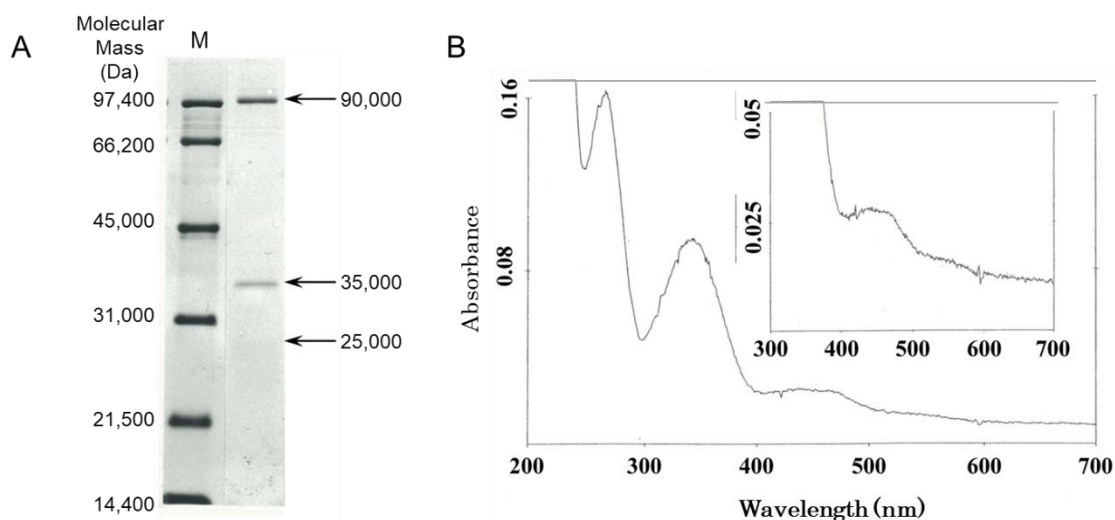


Fig. 2-3 SDS-PAGE and UV-Vis spectrum of purified UTDH.

Table 2-2 Purification of UTDH from *Rhodococcus erythropolis* JCM 3132

Step	Total protein (mg)	Total activity ($\mu\text{mol}/\text{min}$)	Specific activity ($\mu\text{mol}/\text{min}/\text{mg}$)	Recovery (%)	Fold
Cell-free extracts	323	8.58	0.027	100	1
DEAE-sephacel	39.0	20.6	0.53	240	20
Phenyl-sepharose	4.20	10.1	2.40	117	89
Superdex S-200	1.00	8.38	8.38	98	310
MonoQ HR 5/5	0.25	2.25	9.00	26	330
Superose S-6	0.10	0.86	8.60	10	320

Purification buffer: 25 mM Borate/NaOH with 0.1 mM NADPH and 0.1 mM DTT, pH 11.8

Gene cloning and sequencing

UTDH's N-terminal and internal amino acid sequences were obtained. The N-terminal amino acid sequence of the M-subunit was MKPSPLTYHRPSSVEDA and the internal amino acid sequences of the L-subunit were IGKPIPREEDTRLLSGQGGRYLDDLGHNA, AATGLTTQGQGHQTAFQAIVADDLGVK, and VSDVEIVTGDTRRFYAVGTFASRGAVMSGSAFHVA. These amino acid sequences showed significant homologies with those of carbon monoxide dehydrogenase (CODH from *Pseudomonas carboxydovorans*), xanthine dehydrogenase (XDH from *Sulfolobus solfataricus*), nicotine dehydrogenase (NDH from *Arthrobacter nicotinovorans*), and quinoline 2-oxidoreductase (from *Pseudomonas putida*).

Using degenerate primers derived from the internal peptide sequences of UTDH, the UTDH

gene fragments were amplified by PCR. Based on the gene sequences of these fragments, the complete sequence of three ORFs was obtained (total length of 4,069 bp) by the inverse PCR approach. The complete gene and amino acid sequences of UTDH were determined (AB250759.1). The FAD-binding sites, GGQSL and LGGS, were found in the amino acid sequence of the M-subunit. Two [2Fe-2S] cluster binding motifs, C-X4-C-X2-C-Xn-C and C-X2-C-Xn-C-X1-C, were found in the amino acid sequence of the S-subunit (Wang et al. 2016). The molybdenum-binding consensus sequence, GGGFG, in the amino acid sequence of the L-subunit, is a dinucleotide-binding motif assigned to the molybdopterin cytosine dinucleotide (MCD)-type molybdenum cofactor.

Homologous expression of UTDH

SDS-PAGE of recombinant *R. erythropolis* expressing UTDH showed gene expression of 3 subunits of UTDH (Fig. 2-4). However, the recombinant *R. erythropolis* showed no activity if metal solution described in Materials and methods was not added to culture medium. The addition of metal solution was necessary for the active expression of UTDH.

As a result of HPLC analysis, *R. erythropolis* expressing UTDH produced barbituric acid from uracil, but not the vector control (Fig. 2-5). Therefore, the UTDH candidate gene (Accession number: AB250759.1) was confirmed to be the UTDH gene.

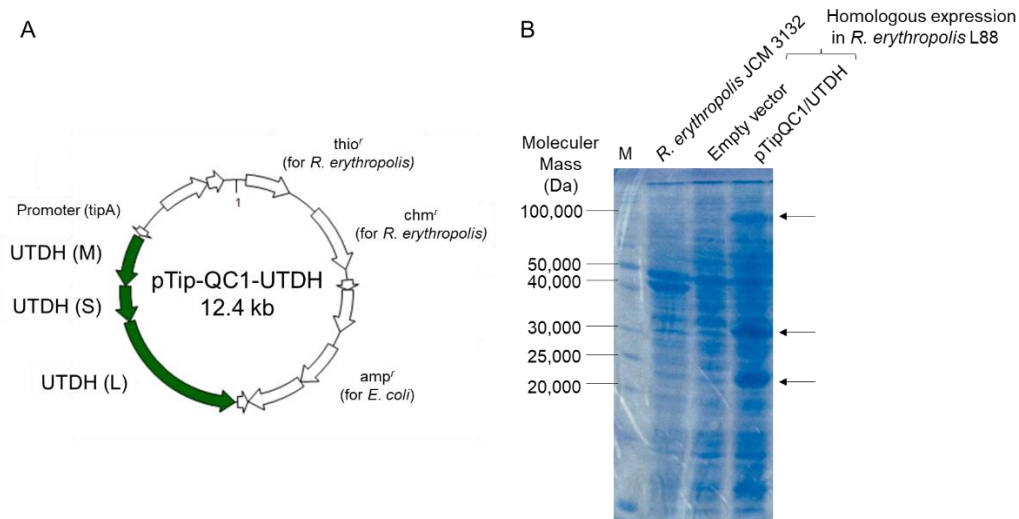


Fig. 2-4 Homologous expression of UTDH by pTip vector

A: Vector map of pTip-QC1-UTDH for homologous expression. B: SDS-PAGE analysis of CFE of *R. erythropolis* L88 expressing UTDH.

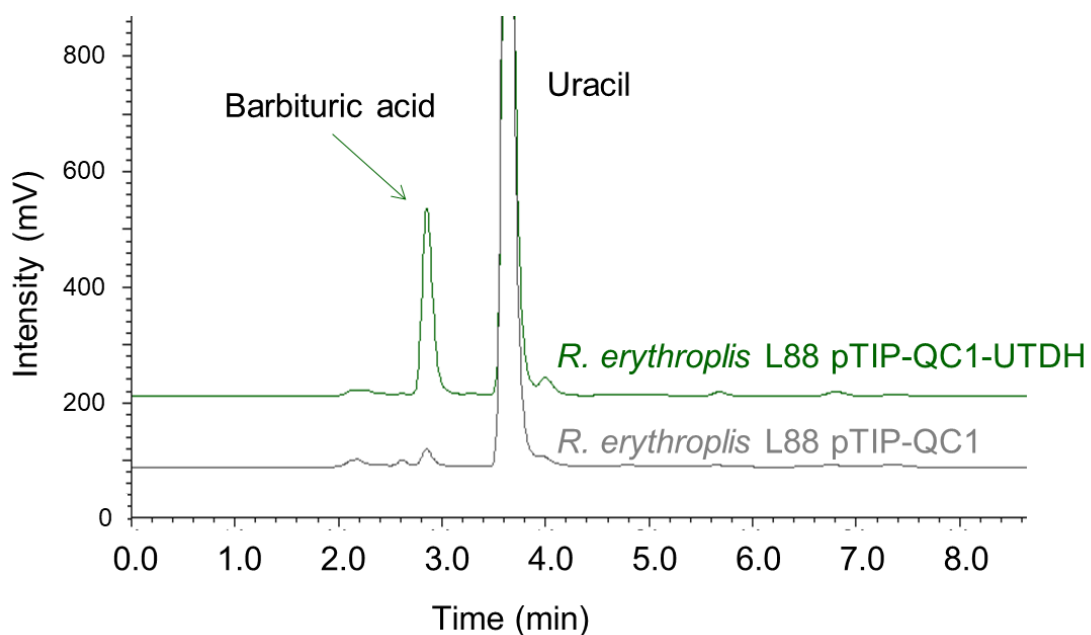


Fig. 2-5 HPLC analysis of reaction mixture incubated with CFE of *R. erythroplis* L88 expressing UTDH

Effects of pH and temperature

UTDH activity and stability were confirmed in sodium acetate, potassium phosphate, Tris/HCl, HEPES/NaOH, borate/NaOH, and glycine/NaOH buffer systems (100 mM), at pH 5.0, 7.0–8.0, 7.5–9.2, 7.0–8.0, 9.0–10.2, and 9.0–10.7, respectively, using purified enzyme. The activity was highest in Tris/HCl buffer, pH 7.5 and 8.5 (Fig. 2-6C). When the enzyme was incubated at 30 °C for 30 min at pH 6.5–12.0, more than 80 % of the initial activity was retained (Fig. 2-6D). The initial velocity of the oxidation of uracil increased with temperature, reaching a maximum at 50 °C (Fig. 2-6A). More than 80 % of the initial activity was retained when the enzyme was incubated at pH 8.0 for 30 min at temperatures lower than 50 °C (Fig. 2-6B).

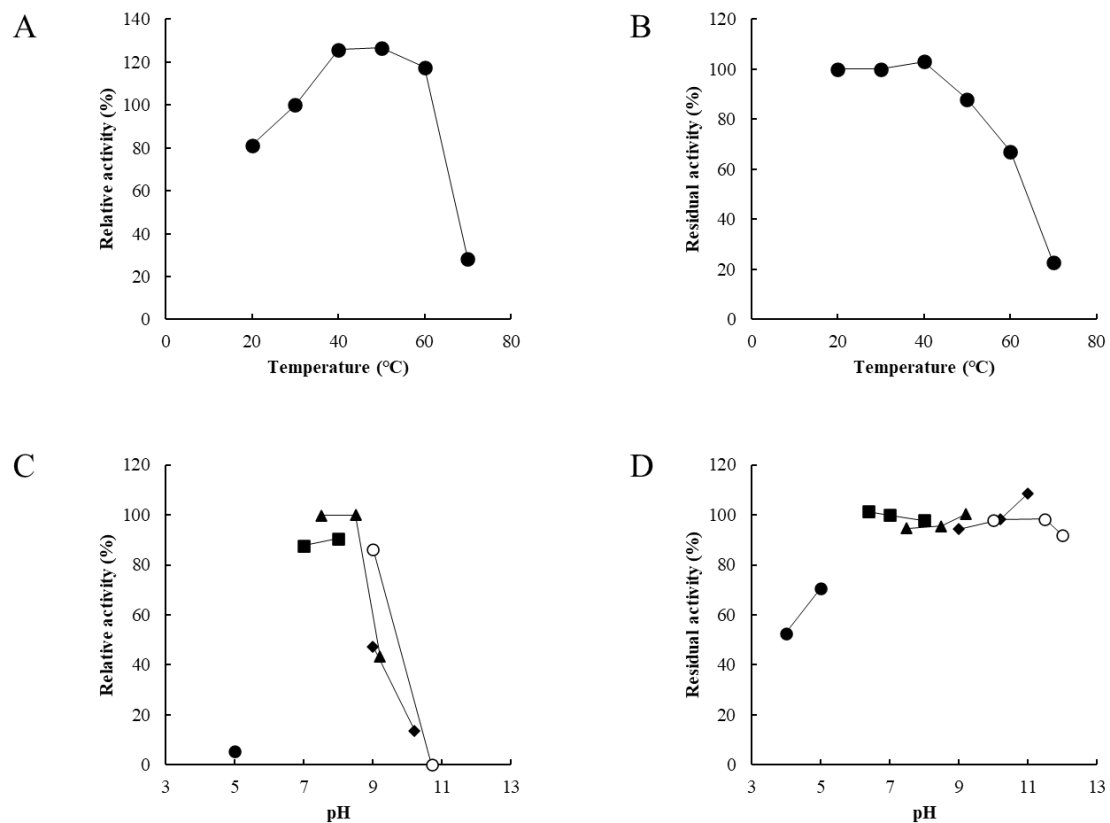


Fig. 2-6 Effect of reaction temperature and pH on activity and stability of UTDH

A. Effect of reaction temperature B. Thermal stability C. Effect of pH. Sodium acetate (pH 5.0), closed circle; potassium phosphate (pH 7.0–8.0), closed square; Tris/HCl (pH 7.5–9.2), closed triangle; borate/NaOH (pH 9.0–10.2), closed diamond; glycine/NaOH (pH 9.0–10.7), open circle. D. pH stability. Sodium acetate (pH 4.0–5.0), closed circle; potassium phosphate (pH 6.4–8.0), closed square; Tris/HCl (pH 7.5–9.2), closed triangle; borate/NaOH (pH 9.0–11.0), closed diamond; glycine/NaOH (pH 10.0–12.0), open circle.

Substrate specificity and kinetic constants

The purified enzyme catalyzed the oxidation of uracil and thymine as well as 5-substituted uracils and 4-(3*H*)-pyrimidone (Table 2-3). The following compounds were not transformed by the purified enzyme: dihydrouracil, dihydrothymine, dihydroorotate, orotate, cytosine, barbiturate, 6-azauracil, 6-methyluracil, 6-aminouracil, xanthine, and nicotine. The K_m , V_{max} , and V_{max}/K_m values for uracil were 0.83 (mM), 8.5 ($\mu\text{mol}/\text{min}/\text{mg}$), and 10.24, respectively. The K_m , V_{max} , and V_{max}/K_m values for thymine were 0.71 (mM), 8.3 ($\mu\text{mol}/\text{min}/\text{mg}$), and 11.69, respectively.

Table 2-3 Substrate specificity and kinetic contents of UTDH

Substrate (5 mM)	Relative activity (%)	K_m (mM)	V_{max} ($\mu\text{mol}/\text{min}/\text{mg}$)	V_{max}/K_m
Uracil	100	0.83	8.5	10
Thymine	70	0.71	8.3	12
5-Ethyluracil	4	-	-	—
5-Propyluracil	20	-	-	—
5-Fluorouracil	23	-	-	—
5-Chlorouracil	30	-	-	—
5-Bromouracil	19	-	-	—
5-Trifluoromethyluracil	19	-	-	—
5-Nitrouracil	2	-	-	—
4-(3 <i>H</i>)-Pyrimidone	6	-	-	—

Reactions were performed using the standard enzyme assay conditions (described in Materials and Methods) but varying substrates.

Effects of inhibitors and metal ions

Enzyme activity was assayed under standard conditions in the presence of various enzyme inhibitors and metal ions (2 mM; Table 2-4). Among the SH-reagents tested, *p*-chloromercuribenzoate and sodium arsenate completely inhibited enzyme activity, while iodoacetate, *N*-ethylmaleimide, and 5,5'-dithiobis (2-nitrobenzoate) showed 11, 50, and 73 % inhibition, respectively. As for metal-binding reagents, KCN and NaN_3 showed 98 % and 66 % inhibition, respectively. The enzyme was sensitive to metal ion chelators such as *o*-phenanthroline (1,10-phenanthroline), α, α' -dipyridyl (2,2'-bipyridyl), and 8-hydroxyquinoline (8-quinolinol). Enzyme activity was inhibited by Cu^{2+} , Zn^{2+} , Co^{2+} , Cd^{2+} , Hg^{2+} , and Pd^{2+} , while it was enhanced by Ce^{4+} . The following metals had no effect on UTDH activity: K^+ , Cs^+ , Rb^{2+} , Ca^{2+} , Mn^{2+} , Mg^{2+} , Be^{2+} , Sr^{2+} , Cr^{3+} , Mo^{6+} , La^{3+} , Nd^{3+} , Sm^{3+} , and Pr^{3+} .

Table 2-4 Effect of inhibitors and metal ions on UTDH activity

Compound (2 mM)	Relative activity (%)
None	100
SH-reagent	
Iodoacetate	89
<i>p</i> -Chloromercuribenzoate	0
<i>N</i> -Ethylmaleimide	50
5-5' -Dithiobis(2-nitrobenzoate)	27
Sodium arsenate	0
Carbonyl reagent	
NH ₂ OH	32
Hydrazine	52
Metal-binding agents	
KCN	2
NaN ₃	34
Metal ion chelator	
EDTA	109
<i>o</i> -phenanthroline	86
α,α' -Dipyridyl	79
8-Hydroxyquinone	50
Metal ion	
CuSO ₄	6
ZnSO ₄	16
CoCl ₂	5
CdCl ₂	65
HgCl ₂	0
PbCl ₂	53
Ce(SO ₄) ₂	156

Reactions were performed using the standard enzyme assay conditions (described in Methods) with listed compounds (2 mM). The following metals had no effect on activity of UTDH: KCl, CsCl, RbCl, CaCl₂, MnCl₂, MgCl₂, BeSO₄, SrCl₂, CrCl₃, and Na₂MoO₄.

Effect of cerium ions

Because UTDH activity was enhanced in the presence of tetravalent cerium ions, the effect of trivalent cerium ions was investigated (Table 2-5). The largest increase in activity was observed with 0.5 mM CeCl₃.

Enzyme activity in the presence of 0.5 mM CeCl_3 was further evaluated with various electron acceptors and substrates (Table 2-6). Using uracil as the substrate and methylene blue, phenazine methosulfate, benzoquinone, or α -naphthoquinone as the electron acceptor, the addition of CeCl_3 increased the enzyme activity in the range of 1.6- to 5.4-fold. With methylene blue as the electron acceptor and uracil, thymine, or 5-fluorouracil as the substrate, the addition of CeCl_3 increased the activity in the range of 2.5- to 5.3-fold.

The time course of the reaction in the presence of CeCl_3 (0.5 mM) was monitored using uracil and methylene blue as the substrate and the electron acceptor, respectively. With the decrease in the substrate, the reaction velocity decreased in the absence of CeCl_3 . While in the presence of CeCl_3 , this decrease in the reaction velocity was not observed, and the initial velocity of the reaction was maintained during the reaction (Fig. 2-7).

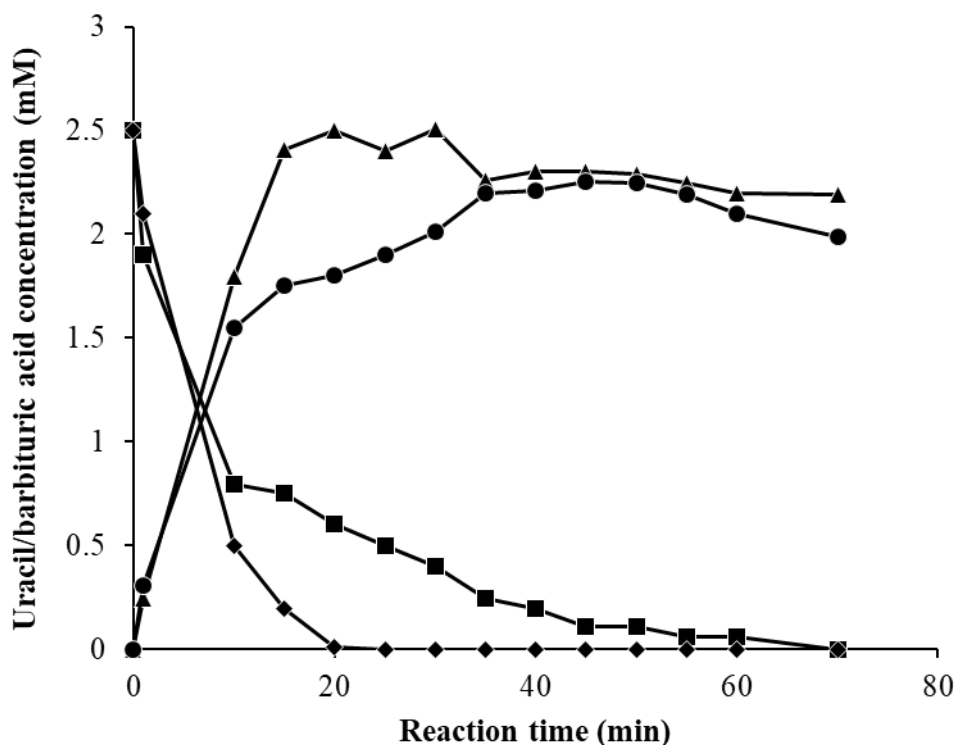


Fig. 2-7 Time course of UTDH reaction in the presence of Ce^{3+} .

Reactions were carried out using the standard enzyme assay conditions in the presence or absence of CeCl_3 (0.5 mM). The triangle depicts barbituric acid production in the presence of Ce^{3+} . The circle depicts barbituric acid production in the absence of Ce^{3+} . The square depicts uracil consumption in the absence of Ce^{3+} . The diamond depicts uracil consumption in the presence of Ce^{3+} .

Table 2-5 Comparison of Ce³⁺ and Ce⁴⁺ on UTDH activity

Cerium ion	Relative activity (%)
None	100
CeCl ₃ ·7H ₂ O (1 mM)	158
CeCl ₃ ·7H ₂ O (0.5 mM)	175
Ce(SO ₄) ₂ ·4H ₂ O (1 mM)	160
Ce(SO ₄) ₂ ·4H ₂ O (0.5 mM)	164

Reactions were performed using the standard enzyme assay conditions (described in Methods) with different forms and concentrations of cerium ions. A decrease in the amount of substrate without Ce³⁺ or Ce⁴⁺ was defined as 100 %.

Table 2-6 Effect of cerium ions on UTDH activity

Electron acceptor test			Substrate test		
Cerium ion (0.5 mM)	-	+	Cerium ion (0.5 mM)	-	+
Electron acceptor	Relative activity (%)		Substrate	Relative activity (%)	
Methylene blue	100	316	Uracil	100	388
Phenazine methosulfate	100	539	Thymine	100	533
Benzoquinone	100	159	5-Fluorouracil	100	250
α-Naphthoquinone	100	191			

Reactions were performed using standard assay conditions (described in Methods).

In the electron acceptor test, uracil was fixed as the substrate. In the substrate test, methylene blue was fixed as an electron acceptor. The amount of the product without Ce³⁺ was defined as 100 %.

Discussion

The information on oxidative pyrimidine metabolism available has been limited (Hayaishi & Kornberg, 1952; Lara, 1952), and the physiological properties of each enzyme involved in the metabolism have not yet been revealed. *R. erythropolis*, a microorganism that assimilates uracil as a carbon source, is a potent organism for the analysis of pyrimidine metabolism. Preliminary studies on metabolism using the CFE of this strain revealed that NAD(P)H didn't enhance uracil decomposition and urea was a degradation product of uracil via barbituric acid as an intermediate. Based on these observations, it was hypothesized that pyrimidine was assimilated through the oxidative pathway in this organism. In chapter 2-1, the detailed physicochemical properties of UTDH that catalyze the first step of its metabolism were described.

A challenge of this UTDH study was the instability of the enzyme; thus, the conditions for stabilizing UTDH were firstly established. The conditions that were established were unusual in that the enzyme required alkaline conditions (pH 11.6) and NADP⁺ as a stabilizer. These conditions, while

not optimal for the activity, enabled us to purify UTDH. The highly alkaline conditions may contribute to stabilizing UTDH by suppressing the activity of other enzymes, including proteases. Additionally, NADP⁺ may contribute to enzyme stabilization by assisting in UTDH complex formation because it is not involved in the reaction. The role of these conditions in UTDH stability will be of interest for further research.

It was found that artificial electron acceptors such as methylene blue are required for UTDH activity. These are electron acceptors with a positive redox potential, and it is possible that electron acceptors with a positive redox potential, such as quinones, are involved in reactions *in vivo*.

The genes of UTDH are located in 6,126,824..6,129,346 (L-subunit), 6,129,343..6,129,987 (S-subunit), and 6,129,990..6,130,892 (M-subunit), and these are far from any genes involved in the biosynthesis of nucleobases, such as aspartate carbamoyltransferase catalytic subunit (2935360..2936304), dihydroorotase (2936301..2937638), and dihydroorotate dehydrogenase (3203920..3204990). As a result of a blast search based on the sequence of the L-subunit, it was found that the other *Rhodococcus* species, such as *R. kyotonensis* and *R. qingshengii*, had aerobic carbon-monoxide dehydrogenase large subunit (90.7 %, and 99.88 % identity). This indicates that *Rhodococcus* species generally have UTDH activity. Complete gene and amino acid sequences of UTDH were deposited as AB250759.1 in 2008. However, the function of UTDH was not understood at that time, and this paper is the first to report the function of UTDH.

Structural analysis of UTDH indicated that the subunit composition is L₂M₂S₂ or L₂M₂S₁ form, containing 1.7 moles of FAD per mole enzyme (M-subunit), iron-sulfur cluster (S-subunit), and molybdenum (L-subunit). UTDH belongs to the xanthine oxidase family, but none has been reported to catalyze the oxidation of pyrimidine bases. Molybdopterin, FAD, and iron-sulfur clusters are usually associated with these enzymes (Hille et al., 2014). For this type of enzyme, the subunit containing the molybdenum-binding site directly binds to the substrate. Therefore, the L-subunit sequence of UTDH was compared with those from proteins stored in UniProtKB/Swiss-Prot (Swiss-Prot) using BLAST software and revealed significant homology (35 % identity, Fig. 2-8) with caffeine (1,3,7-trimethylxanthine) dehydrogenase in *Pseudomonas* sp. CBB1 (Yu et al., 2008). *Pseudomonas* sp. caffeine dehydrogenase is also a heterotrimer with $\alpha\beta\gamma$ subunits, and the catalytic function of caffeine dehydrogenase is to oxidize the C-8 position and to form 1,3,7-trimethyluric acid. The shared features of UTDH and caffeine dehydrogenase are 1) xanthine is not a substrate, 2) dichlorophenolindophenol, but not NAD(P)⁺, serves as an electron acceptor, and 3) both are heteromeric enzymes with $\alpha\beta\gamma$ subunits. From these observations, UTDH and caffeine dehydrogenase show similar properties among known molybdenum hydroxylases, and it may be of future interest to examine whether *Pseudomonas* caffeine dehydrogenase also catalyzes the oxidation of pyrimidine bases.

Crystal structures of carbon monoxide dehydrogenase (CODH) from *Hydrogenophaga*

pseudoflava (Hänzelmann et al., 2000) and quinoline 2-oxidoreductase (QOR) from *Pseudomonas putida* (Bonin et al., 2004) have been reported. There is the conserved domain to bind the molybdenum cofactor in the xanthine oxidase family. UTDH has the conserved domain as well as the other molybdenum hydroxylases (Fig. 2-8).

As shown in Fig. 2-9, UTDH was found to belong to the molybdenum hydroxylase superfamily based on phylogenetic analysis of the sequence of L-subunit by an unweighted pair-group method with arithmetic mean (UPGMA). This superfamily is divided into eight families as shown in each box in Fig. 2-9. It was revealed that *R. erythropolis* UTDH is categorized into the same group as *Pseudomonas* CODH along with *Pseudomonas* CBB1 caffeine dehydrogenase (Yu et al., 2008). This subfamily shows strict specificity toward electron acceptors. UTDH, like caffeine dehydrogenase, uses methylene blue, phenazine methosulfate, and benzoquinone as electron acceptors, but not NAD⁺, NADP⁺, FAD, FMN, or molecular oxygen. In contrast, several XDHs can use NAD(P)⁺ and molecular oxygen as electron acceptors, despite their L-subunit protein sequence homology with UTDH.

Interestingly, the activity of UTDH was found to be enhanced by cerium ions. This activation was observed with any combination of substrates and electron acceptors. There are several reports concerning the biochemical effects of cerium ions, such as an increase of chlorophyll contents and photosynthetic rate, and hydrolysis of DNA strands (Fashui et al., 2002; Yuguan et al., 2009). Cerium ions can catalyze the hydrolysis of DNA chains like restriction enzymes and can nonenzymatically cleave phosphodiester bonds of DNA as a cerium–EDTA complex (Katada & Komiyama, 2009) or dimer (dicerium) complex (Branum et al., 2001). Revealing the scientific basis of the effect of cerium ions is also of future interest.

```

UTDH 1 MSTPVKPAKRNKAKHPASDHSVADGKFFKPIPREEDTRLLS*QGRMLD*LGHN-AIIA*FVSS*HHARID*IIDQ*LEVGV*HAIY*YV*LLADTFEMAENLPLLPHPGIAPRNGY*FA 129
QOR 1 -----MMKHEVVALK*KSI*GTSLRREDTRLLT*SRGR*ADLVLSGMLH*VASLRS*FAHARIVS*LDVAD*QAL*EGVGL*WVC*GDV*VELSQ*IVAM*QVEG*QT*----TIQ*PLDA 105
CODH 1 -----MNAFVQDAEARELALAGMRPRCAKEDARFIQ*KRGM*VD*IKM*GM*LH*MDI*V*PA*IAH*SR*IKK*HK*DA*LAM*GV*HAVL*TA*BD*LK*PLK*HW*MT*LAGD*-----VA*AVDA 104
CaDH 1 -----MFAD*IN*KGDA*FG*TW*GK*VP*FR*EDAD*IL*A*RAE*MA*IK*LP*GM*EA*AF*LS*FA*HARIVS*LDV*S*AL*AI*EG*Y*DM*V*GP*IP*DY*V*K*PL*PL*M*ITY*Q*NH*RE*----I*PT*SDA 106
XDH 1 -----MRVDA*LAK*VT*SR*AR*DT*DDY*MAG*CY*AK*VS*LS*IA*HS*YAVS*INDE*Q*AR*SL*EG*VL*AI*TF*W*ED*VP*DF*PA*TAG*HAW*TLD*ENK*---RD*AD*R*ALL 89

UTDH 130 KDEV*KH*VEA*IN*W*ND*RY*LD*ED*CA*KID*V*YEA*K*PV*VG*LD*V*RTA*AN*VH*AD*VPD*N-----VA*AHL*Q*H*GF*DL*DA*EL*AA*PH*RL*LD*LEI*ERS*AS*SM*PE*GK*GV*AR*W*GD*ENT*L*TWT 245
QOR 130 NGV*RF*VE*IV*W*AS*SR*AL*ED*DA*QL*LV*VE*YEP*PA*VT*GE*AL*EG*-EAR*AND*TLAGN-----V*VS*RS*RR*AR*DEL*AF*IF*AS*AG*V*RG*FC*GR*VS*AD*FC*GR*VA*LEN*RS*IT*DG*AM*N*LP*W*Q*LV*ESH*VGN*AVIL 221
CODH 105 DEK*VE*H*Q*CV*VA*IN*AD*RY*AD*AV*EA*V*KE*VE*YEP*PV*VID*P*ID*AL*K*P*DA*PV*LR*ED*L*AG*TS*GA*H*GR*EH*HN*IF*TW*AG*DK*AA*DA*V*FA*NA*EV*YS*Q*H*MY*RV*H*PC*PE*CC*GV*AS*FP*IK*GD*L*ITY*I 234
CaDH 107 RDI*V*RY*AGE*EV*W*AIN*RY*V*AD*LE*L*LV*VE*YEP*PV*VAS*ID*AS*LA*VD*GP*RL*YEG*W*PD*N-----V*VAK*VS*SEI*GV*DA*MA*S*AD*LV*FE*ER*FEI*QR*CH*PA*LE*TR*GF*LD*Q*W*DF*K*GEN*LV*WN 223
XDH 90 TRH*VR*HH*GD*AV*IV*AR*DEL*T*SK*RA*QL*V*SI*EW*QEP*LV*ITT*PE*AL*AE*DA*PI*H*NGGN-----L*L*Q*ST*M*ST*GN*V*Q*TI*DA*AV*Q*H*Y*QT*F*VI*QH*CH*ES*VT*LS*W*ME*-DD*S*RI*TVS 203

UTDH 246 S*PC*TS*S*AR*AA*IA*AR*GM*AL*N*K*HC*IA*ED*V*GG*GF*GV*KI*V*HP*WE*EV*MI*TWA*ARR*L*G*AG*IS*CV*KW*VE*DR*SE*HI*SSA*HE*RG*Q*IK*V*DI*GF*DD*ER*LL*AF*DF*TF*WH*D*NG*AM*LP*Y*GI*VM*IN*---TAT*Q*VL 372
QOR 222 AR*OM*FS*RV*FM*VM*FA*IC*EH*LE*VR*VE*VD*V*GG*GF*CV*KA*HL*HE*PELL*V*CL*L*SR*AL*GR*-----V*RV*IE*DR*EN*EL*G*A*TH*A*K*Q*RV*NE*MG*LA*FD*GR*FL*AL*EN*RS*IT*DG*AM*N*LP*W*Q*LV*ESH*VGN*AVIL 345
CODH 235 TS*CA*EH*VR*VR*VM*SL*GS*IE*SK*VR*IV*SE*DI*V*GG*GF*CV*NK*VG*I*Y*EG*CV*IA*V*AS*IV*L*GR*-----V*KW*VE*DR*EN*IS*T*AF*AR*D*Y*HM*DE*LA*AT*FG*KL*L*GR*V*N*V*AD*GF*AD*CAD*PT*K*FP*AG*L*PH*ICS- 357
CaDH 224 G*VL*IE*NAR*SV*AK*IV*ND*K*PE*SG*-SY*R*GW*Q*-P*QAN*FA*VR*VM*LL*AR*QL*DP*AA*VR*IN*Y*VE*-AR*MP*T*G*-LA*HT*FD*-----S*GR*EV*L*H*DR*AL*K*TF*Y*EAW*LER*Q*AA*Q*GR*----I*CH*MS*FY 345
XDH 204 S*PC*TH*VR*VS*Q*AL*DE*WS*CV*RV*IR*SE*V*GG*GF*CV*NK*Q*DL*VE*EP*MA*AF*IT*SK*L*GG*IE*-----V*KV*SL*SE*EE*CLA*TR*HA*FT*IG*CM*V*NR*DT*L*K*Y*SL*DL*VL*SN*TV*SA*SH*GH*SA*SAG*---GN*KVA 324

UTDH 373 G*PK*PK*SR*VN*AY*SL*IN*TV*IT*-PY*R*AG*R*-P*QAV*FAM*R*SM*DA*IK*RY*KN*K*IA*V*REAN*F*TR*-ED*MD*DF*L*MF*Q*DR*PL*IY*DT*GD*Y*Q*AG*ID*K*L*K*L*ID*WD*GF*PEY*QR*KAR*AG*SS*---V*H*IG*AY 496
QOR 346 G*VE*K*VE*AV*SE*SI*AV*AN*K*CE*IG*-AY*R*SV*GF*-TAG*Q*IA*R*BT*L*DR*AR*CH*LS*FE*RR*RV*MP*-ED*FE*T*NR*L*GG*THR*-----E*GT*ML*Q*T*IN*LE*EM*VN*PE*FR*QR*CA*EAR*AG*KY*----L*EL*GV*VE 421
CODH 358 G*SD*IP*RA*HC*SV*K*GV*IN*K*AE*GV*VA*CS*FR*VE*AY*YL*ER*MD*V*VL*AK*ND*K*AE*RA*K*F*TR*-EQ*FE*TT*Q*FG*FEY*-----S*GD*Y*HT*AL*K*V*LD*AV*Y*PA*WR*AE*Q*AR*AD*PNS*PT*LM*CH*LV*TE 480
CaDH 346 G*VL*IE*NAR*SV*AK*IV*ND*K*PE*SG*-SY*R*GW*Q*-P*QAN*FA*VR*VM*LL*AR*QL*DP*AA*VR*IN*Y*VE*-AR*MP*T*G*-LA*HT*FD*-----S*GR*EV*L*H*DR*AL*K*TF*Y*EAW*LER*Q*AA*Q*GR*----I*CH*MS*FY 462
XDH 325 Y*LR*CA*Y*AYS*SK*TY*IN*LF*SAG*-AV*R*Y*GA*-P*QV*FA*VE*SM*LD*AT*AL*GI*DE*VR*LR*AA*RE*GDAN*EL*T*G*K*RY*SAG*-----L*PE*CL*E*GR*K*IF*EW*E*K*RA*E*C*Q*N*QL*RR*----I*CH*V*ACE 439

UTDH 497 V*EG*TS*PE*-----P*Y*EG*A*H*V*VE*TS*AV*KA*A*T*GL*TT*CG*GH*TA*FA*CT*V*AD*L*V*K*VS*D*VE*IV*T*GD*TR*-FG*Y*AV*CF*FA*R*SA*VM*SS*AF*PH*AA*Q*VA*ER*K*AK*IS*GI*DL*PETE*LE*RE*SH*V 612
QOR 464 ND*CT*GT*E*-T*RL*SL*FL*PT*TT*H*SA*TV*RI*DP*TR*AV*TF*EL*ASS*CG*HE*TT*L*AC*AD*VL*VE*AS*D*W*V*Q*AS*TKN*-TY*GF*AY*AR*SA*VI*GAG*IG*RA*AS*IV*RE*RV*K*QL*SH*LE*AA*SE*DI*VI*ED*GL* 590
CODH 461 TE*V*VE*AS*ES*K*MD*IL*G*--V*GM*FE*SC*IR*L*HP*TS*AL*ARM*GT*TC*CG*GH*TY*ACT*IT*LE*IE*SE*V*Q*VE*SD*TS*-AP*Y*GL*SV*GR*ST*VA*GA*IAL*AA*K*HA*K*AK*TA*AM*GV*EN*MD*L*W*VD*RF 607
CaDH 463 AE*VS*AR*SES*RF*LV*GG*Q*GG*Y*IA*RI*RM*DT*GD*W*Y*TE*GC*CM*CG*VT*NS*L*GL*AD*AL*CL*NP*DD*VT*WG*ST*AL*NP*Y*TW*EG*ARS*IT*IG*FA*VM*AP*RL*RE*K*LS*AR*W*LD*AD*PD*L*VL*AN*RG 592
XDH 440 SY*TS*NT*W*VE*G*-----V*E*TAG*AR*LL*M*N*Q*ET*IN*V*QS*GA*TE*CG*CA*DT*VE*GV*AV*ET*VE*VS*DR*VI*ST*Q*DT*VT*FD*FA*FA*RS*SY*VA*AF*LR*SL*LL*L*K*K*II*A*HR*VM*H*QS*AM*V*L*L*K*SH*I 560

UTDH 613 CK*IE*TEA*GV*EG*TS*V*PL*SV*AV*LS*VN*PL*RY*AF*DR*ES*K*LAT*G*FA*K*TD*D*MS*K*FP*I*EE*EQ*DF*ER*GY*ES*FS*TS*CS*V*HAA*IV*ET*Y*TA*EIT*VR*Y*V*I*HP*GV*N*V*AV*Y*GV*GV*AV*AG*IG*AL*Y*R 742
QOR 591 HV*AG*VEA*-----K*GM*F*EV*V*GA*Y*FAD*AT*HP*FS*DA*TD*ER*AT*Y*DS*DL*VAN*GS*HAA*IV*EL*AST*Y*ATR*Y*TD*FA*VE*CG*TR*EN*W*IV*SG*IR*SH*IA*Q*AL*GT*LL*EE 694
CODH 608 KV*GG*DD*S*-----K*FT*M*AD*IA*W*Q*Y*HQ*---P*AG*LE*FE*ED*Y*HW*Y*DE*EN*TY*PE*CY*LV*CV*DR*AT*GET*K*WR*RY*AL*DR*CT*RM*EN*IV*IG*HE*SL*TE*SY*AV*AM*QQ 708
CaDH 593 MR*DD*EG*-----R*Y*VS*FS*I*G*RA*Y*Q*IL*EL*ED*VE*EE*GV*VE*FT*V*QL*AW*FP*GN*L*VAV*VE*ED*GV*AV*SL*CM*L*W*H*EP*IN*W*EN*IV*Y*GL*PE*SH*IQ*GL*QA*L*Y*EE 696
XDH 561 VL*VER*EE*-----E*PL*MS*L*K*DL*AMD*RF*Y*HP*---E*RG*GL*SD*SS*IK*TT*NP*IE*CF*VD*LV*IAL*CK*VT*IN*IL*N*W*HS*SH*IL*N*W*EL*AE*CG*VE*GM*GI*W*AL*FE* 660

UTDH 743 IV*Y*EH*-Q*ML*NAS*Y*MD*FL*MP*FV*EM*Q*SL*EM*D*HT*VP*SG*LN*PL*VE*SG*AG*VI*PTS*V*IA*AM*EP*AG*IS*TS*MP*IS*PS*EL*FE*LR*L*AH*AG*SS*SE*ENA 840
QOR 695 VLY*DF*-Q*LV*TT*IT*MD*FL*PL*DL*VD*-IR*IR*HE*TP*SEL*VP*GC*IK*GM*ES*SAM*SAP*AN*AV*AN*VD*LA*HL*-V*VI*ET*VE*IE*FR*IS*Q*ER*RM*Q*-- 788
CODH 709 MP*FA*Q*-NIL*GN*TL*MD*FL*PA*VE*TE*H*-WE*D*HT*VP*SP*HH*PI*AK*GV*AS*PH*VS*IP*TT*PA*AV*DA*FA*H*V*-V*TH*LD*M*HS*Y*RV*WS*L*K*EH*N*L*AL- 803
CaDH 697 LNV*EN*-Q*IG*YS*G*FA*DL*MP*AS*EL*EN*-MR*F*D*H*W*VE*SE*PL*IG*MS*GV*VE*SG*TE*PA*V*AV*EN*EN*LR*PI*NS*KL*NR*ET*VE*ED*RL*TA*IS*AG*ACA-- 791
XDH 661 MII*AK*SV*VR*N*FM*LD*IK*ME*MD*LE*Q*-LE*S*AF*VE*INE*QS*AY*SR*SL*GP*PI*EP*---VA*AR*NR*W*K*MA*GV*AIN*TL*EL*TE*K*RY*EE*FH*LAG*L-- 752

```

Fig. 2-8 Comparison of the amino acid sequence of UTDH L-subunit with those of QOR, CODH, CaDH, and XDH.

Alignment was performed with the GENETYX 11 program. Gaps denoted by *dashes* were inserted to obtain maximum homology. Conserved residues are indicated by gray (50 %) and black (100 %) background. UTDH, uracil-thymine dehydrogenase from *R. erythropolis* JCM 3132; QOR, quinoline 2-oxidoreductase from *Pseudomonas putida* (P7224); CODH, carbon monoxide dehydrogenase from *Hydrogenophaga pseudoflava* (P19913); CaDH, caffeine dehydrogenase from *Pseudomonas* sp. Strain CBB1 (Swiss-Prot, D7REY3); XDH, xanthine dehydrogenase from *E. coli* (Swiss-Prot, Q46799). The *Q248 and motifs I to V interact with the molybdenum cofactor (Hanzelmann et al. 2000). **The active-site loop.

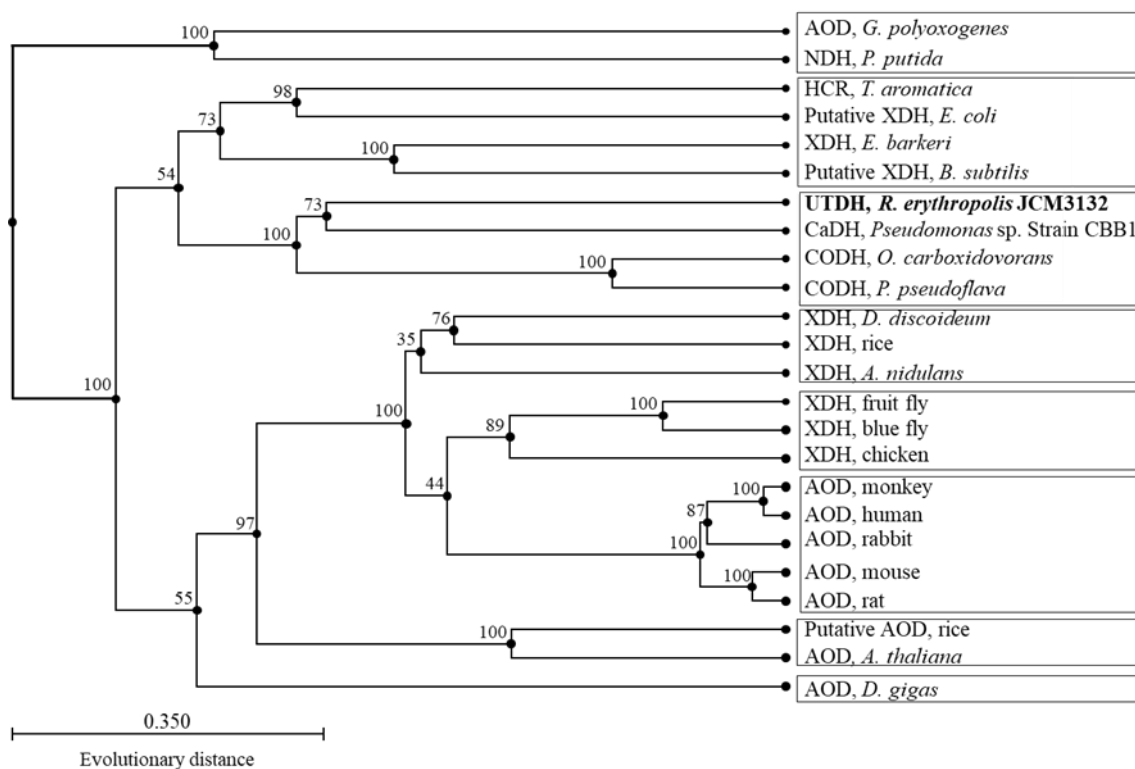


Fig. 2-9 Phylogenetic tree for molybdenum hydroxylases.

The tree was constructed by the UPGMA procedure using the CLC sequence viewer 6.9 (CLC bio, Denmark) based on the amino acid sequence of L-subunit. There are eight main families from an evolutionary standpoint as shown in boxes. AOD, aldehyde oxidase; NDH, nicotine dehydrogenase; HCR, 4-hydroxybenzoyl-CoA reductase; CODH, carbon monoxide dehydrogenase; XDH, xanthine dehydrogenase. All sequences are retrieved from the Swiss-Prot database, and the accession number for each sequence is given in parentheses: AOD, *Gluconacetobacter polyoxogenes*, (P17201); NDH, *Pseudomonas putida* (Q88FX8); HCR, *Thauera aromatica* (O33819); putative XDH, *Escherichia coli* (Q46799); XDH, *Eubacterium barkeri* (Q0QLF2); putative XDH, *Bacillus subtilis* (O32144); UTDH, *Rhodococcus erythropolis* (this study); CaDH, *Pseudomonas sp.* strain CBB1 (D7REY3); CODH, *Oligotropha carboxidovorans* (P19919); CODH, *Pseudomonas pseudoflava* (P19913); XDH, *Dictyostelium discoideum* (Q54FB7); XDH, rice (Q6AUV1); XDH, *Aspergillus nidulans* (Q12553); XDH, fruit fly (P10351); XDH, blue fly (P08793); XDH, chicken (P47990); AOD, monkey (Q5FB27); AOD, human (Q06278); AOD, rabbit (P80456); AOD, mouse (O54754); AOD, rat (Q9Z0U5); putative AOD, rice (Q6Z351); AOD (indole-3-acetaldehyde oxidase), *Arabidopsis thaliana* (Q7G193); AOD, *Desulfovibrio gigas* (Q46509).

The values at the branch are local bootstrap probability, which is the rough reliability of its branch.

References

- Andersson Rasmussen, A., Kandasamy, D., Beck, H., Crosby, S. D., Björnberg, O., Schnackerz, K. D., & Piškur, J. (2014). Global Expression Analysis of the Yeast *Lachancea* (*Saccharomyces*) *kluyveri* Reveals New *URC* Genes Involved in Pyrimidine Catabolism. *Eukaryotic Cell*, *13*(1), 31–42. <https://doi.org/10.1128/EC.00202-13>
- Bonin, I., Martins, B. M., Purvanov, V., Fetzner, S., Huber, R., & Dobbek, H. (2004). Active Site Geometry and Substrate Recognition of the Molybdenum Hydroxylase Quinoline 2-Oxidoreductase. *Structure*, *12*(8), 1425–1435. <https://doi.org/10.1016/j.str.2004.05.014>
- Branum, M. E., Tipton, A. K., Zhu, S., & Que, L. (2001). Double-Strand Hydrolysis of Plasmid DNA by Dicerium Complexes at 37 °C. *Journal of the American Chemical Society*, *123*(9), 1898–1904. <https://doi.org/10.1021/ja0010103>
- Fashui, H., Ling, W., Xiangxuan, M., Zheng, W., & Guiwen, Z. (2002). The Effect of Cerium (III) on the Chlorophyll Formation in Spinach. *Biological Trace Element Research*, *89*(3), 263–276. <https://doi.org/10.1385/BTER:89:3:263>
- Hänzelmann, P., Dobbek, H., Gremer, L., Huber, R., & Meyer, O. (2000). The effect of intracellular molybdenum in *Hydrogenophaga pseudoflava* on the crystallographic structure of the selenomolybdo-iron-sulfur flavoenzyme carbon monoxide dehydrogenase. *Journal of Molecular Biology*, *301*(5), 1221–1235. <https://doi.org/10.1006/jmbi.2000.4023>
- Hayaishi, O., & Kornberg, A. (1952). Metabolism of cytosine, thymine, uracil, and barbituric acid by bacterial enzymes. *The Journal of Biological Chemistry*, *197*(2), 717–732.
- Hille, R., Hall, J., & Basu, P. (2014). The Mononuclear Molybdenum Enzymes. *Chemical Reviews*, *114*(7), 3963–4038. <https://doi.org/10.1021/cr400443z>
- Katada, H., & Komiyama, M. (2009). Artificial Restriction DNA Cutters as New Tools for Gene Manipulation. *ChemBioChem*, *10*(8), 1279–1288. <https://doi.org/10.1002/cbic.200900040>
- Lara, F. J. S. (1952). ON THE DECOMPOSITION OF PYRIMIDINES BY BACTERIA II. *Journal of Bacteriology*, *64*(2), 279–285. <https://doi.org/10.1128/jb.64.2.279-285.1952>
- Loh, K. D., Gyaneshwar, P., Markenscoff Papadimitriou, E., Fong, R., Kim, K.-S., Parales, R., Zhou, Z., Inwood, W., & Kustu, S. (2006). A previously undescribed pathway for pyrimidine catabolism. *Proceedings of the National Academy of Sciences*, *103*(13), 5114–5119. <https://doi.org/10.1073/pnas.0600521103>
- Ogawa, J., & Shimizu, S. (1997). Diversity and versatility of microbial hydantoin-transforming enzymes. *Journal of Molecular Catalysis B: Enzymatic*, *2*(4–5), 163–176. [https://doi.org/10.1016/S1381-1177\(96\)00020-3](https://doi.org/10.1016/S1381-1177(96)00020-3)
- Osterman, A. (2006). A hidden metabolic pathway exposed. *Proceedings of the National Academy of Sciences*, *103*(15), 5637–5638. <https://doi.org/10.1073/pnas.0601119103>
- Piškur, J., Schnackerz, K. D., Andersen, G., & Björnberg, O. (2007). Comparative genomics reveals

- novel biochemical pathways. *Trends in Genetics*, 23(8), 369–372. <https://doi.org/10.1016/j.tig.2007.05.007>
- Soong, C.-L., Ogawa, J., Sakuradani, E., & Shimizu, S. (2002). Barbiturase, a Novel Zinc-containing Amidohydrolase Involved in Oxidative Pyrimidine Metabolism. *Journal of Biological Chemistry*, 277(9), 7051–7058. <https://doi.org/10.1074/jbc.M110784200>
- Soong, C.-L., Ogawa, J., & Shimizu, S. (2001). Novel Amidohydrolytic Reactions in Oxidative Pyrimidine Metabolism: Analysis of the Barbiturase Reaction and Discovery of a Novel Enzyme, Ureidomalonase. *Biochemical and Biophysical Research Communications*, 286(1), 222–226. <https://doi.org/10.1006/bbrc.2001.5356>
- Syldatk, C., May, O., Altenbuchner, J., Mattes, R., & Siemann, M. (1999). Microbial hydantoinases - industrial enzymes from the origin of life? *Applied Microbiology and Biotechnology*, 51(3), 293–309. <https://doi.org/10.1007/s002530051395>
- Vogels, G. D., & Van der Drift, C. (1976). Degradation of purines and pyrimidines by microorganisms. *Bacteriological Reviews*, 40(2), 403–468. <https://doi.org/10.1128/br.40.2.403-468.1976>
- Yu, C. L., Kale, Y., Gopishetty, S., Louie, T. M., & Subramanian, M. (2008). A Novel Caffeine Dehydrogenase in *Pseudomonas* sp. Strain CBB1 Oxidizes Caffeine to Trimethyluric Acid. *Journal of Bacteriology*, 190(2), 772–776. <https://doi.org/10.1128/JB.01390-07>
- Yuguan, Z., Min, Z., Luyang, L., Zhe, J., Chao, L., Sitao, Y., Yanmei, D., Na, L., & Fashui, H. (2009). Effects of Cerium on Key Enzymes of Carbon Assimilation of Spinach Under Magnesium Deficiency. *Biological Trace Element Research*, 131(2), 154–164. <https://doi.org/10.1007/s12011-009-8354-5>

Section 2

Heterologous expression and characterization of ureidomalonnase

Abstract

There has been a report on the involvement of ureidomalonnase in the catalysis of amide hydrolysis, which occurs during the third reaction step of the oxidative degradation of pyrimidine. However, to date, there has been no evidence of the identification of its functional gene or protein. In the present study, ureidomalonnase from *Rhodococcus erythropolis* JCM3132 was successfully purified to homogeneity a functional protein from *Escherichia coli* Rosetta2 (DE3) overexpressing the enzyme, and it was shown that this purified enzyme catalyzes the amide hydrolysis of ureidomalonic acid into urea and malonic acid. It was also shown that the enzyme exhibited a strict specificity toward ureidomalonic acid. Importantly, gene expression of the gene cluster of the pyrimidine oxidative degradation pathway was shown to be inducible by the addition of uracil. The pyrimidine oxidative metabolism can be utilized for the production of purine nucleoside. Indeed, it was demonstrated that the pyrimidine oxidative degradation could be useful in the equilibrium control of ribose transfer between pyrimidine and purine bases, with a significant increase in the conversion yield of purine nucleoside synthesis.

Introduction

In living cells, the pyrimidine pools are tightly regulated by control mechanisms such as *de novo* biosynthesis, salvage, and degradation pathways because pyrimidine bases are precursors to DNA and RNA molecule synthesis. In the degradation process, RNA molecules serve as preferential sources compared to DNA. Pyrimidine is known to be degraded through 4 different pathways (Fig. 3-1).

The most studied pathway has been the reductive metabolic pathway, in which pyrimidine is reduced to dihydropyrimidine derivatives by dihydrouracil dehydrogenase in the initial reaction. It is then converted to β -amino acid, ammonia, and carbon dioxide via β -ureidoamino acid as a result of dihydropyrimidinase and ureidopropionase activities (Syldatk et al., 1999; Tsai & Axelrod, 1965; Vogels & Van der Drift, 1976) (Fig. 3-1B). It is well documented that mammals, plants, and microorganisms operate through this pathway.

The pyrimidine utilization (rut) pathway was found in *Escherichia coli* (Loh et al., 2006; Osterman, 2006; Piškur et al., 2007). In the rut pathway, uracil added as a nitrogen source was metabolized into 3-hydroxypropionic acid, ammonia, and CO₂ in the presence of oxygen at room temperature (Fig. 3-1C). Genetic information and metabolic mechanisms associated with the rut pathway have previously been reported (Parales & Ingraham, 2010).

The URC pathway was found in *Lachancea kluyveri* in which uracil is converted to urea via

ribosyl-urea (Andersson Rasmussen et al., 2014) (Fig. 3-1D).

In the oxidative pathway, pyrimidine is oxidized into barbituric acid derivatives by uracil/thymine dehydrogenase (UTDH) in the initial reaction. It is then converted into urea and malonic acid via ureidomalonic acid as a result of barbiturase and ureidomalonase activity (Fig. 3-1B). Investigations on the pyrimidine oxidative metabolism are limited to a single actinomycetes represented by *Rhodococcus erythropolis* (Horinouchi, Soon, et al., 2012; Soong et al., 2001b, 2002). Our study is based on the rationale that *R. erythropolis* assimilates uracil as a carbon source and may thus represent a potent strain for pyrimidine oxidative metabolism. The features of this strain are: 1) an energy-independent degradation of uracil, that is, no requirement of NAD(P)H, and 2) the existence of a conversion of barbituric acid into urea. On the basis of these observations, it was proposed that pyrimidine is assimilated through an oxidative pathway in the *R. erythropolis* strain. Microbial studies revealed that the metabolic activity of this strain differs from that of a pyrimidine reductive pathway. While current knowledge on the pyrimidine oxidative pathway is scarce, the existence of homologous genes involved in pyrimidine oxidative pathway has been reported in *Saccharomonospora* (Kyoto Encyclopedia of Genes and Genomes (KEGG); Svir_20970), *Blastococcus* (KEGG; BLASA_0154), and *Pseudomonas* (GenBank™; AF086815) through recent genomics analysis. This strongly suggests that some microorganisms also possess pyrimidine oxidative metabolism.

Over the past decades, reports on the pyrimidine oxidative pathway have been rare. Although it is a naturally occurring metabolic pathway, knowledge of the oxidative pathway and its biological importance is very limited. The references available on oxidative pyrimidine metabolism showed that pyrimidine bases are initially oxidized to barbituric acid derivatives, which are then further hydrolyzed directly into urea and malonic acid by barbiturase activity (Hayaishi & Kornberg, 1952; Lara, 1952; Wang & Lampen, 1952). Investigations on barbiturase in *R. erythropolis*, however, revealed the activity of another unidentified consecutive enzyme (Soong et al., 2001b). An unknown product derived from the barbiturase reaction was identified, and this product was characterized as follows: 1) it spontaneously cyclized to barbituric acid, 2) it gave no absorption peak around 250 nm, therefore it was considered to be a non-cyclic compound, and 3) it was transformed into urea and malonic acid by another consecutive enzyme. Altogether, these results suggest that the reaction product of barbiturase is ureidomalonic acid and that an unidentified enzyme—which was named ureidomalonase—is responsible for the catalysis of the amidohydrolysis of ureidomalonic acid into urea and malonic acid through the pyrimidine oxidative pathway.

In the context of biotechnology, dihydropyrimidinase in the pyrimidine reductive degradation pathway is well known for its usefulness in synthesis of optically active β -amino acids (Soong et al., 2001a). From a clinical point of view, several reports have documented metabolic disorders associated with pyrimidine metabolisms. However, the clinical symptoms are not severe because pyrimidine metabolites are highly soluble in water. These reasons may explain the relative

delay in furthering the current understanding of pyrimidine metabolism.

This paper described the cloning of its gene into *Escherichia coli*, the purification of ureidomalonnase from *E. coli* overexpressing ureidomalonnase with His-tag as a functional protein, and its functional analysis.

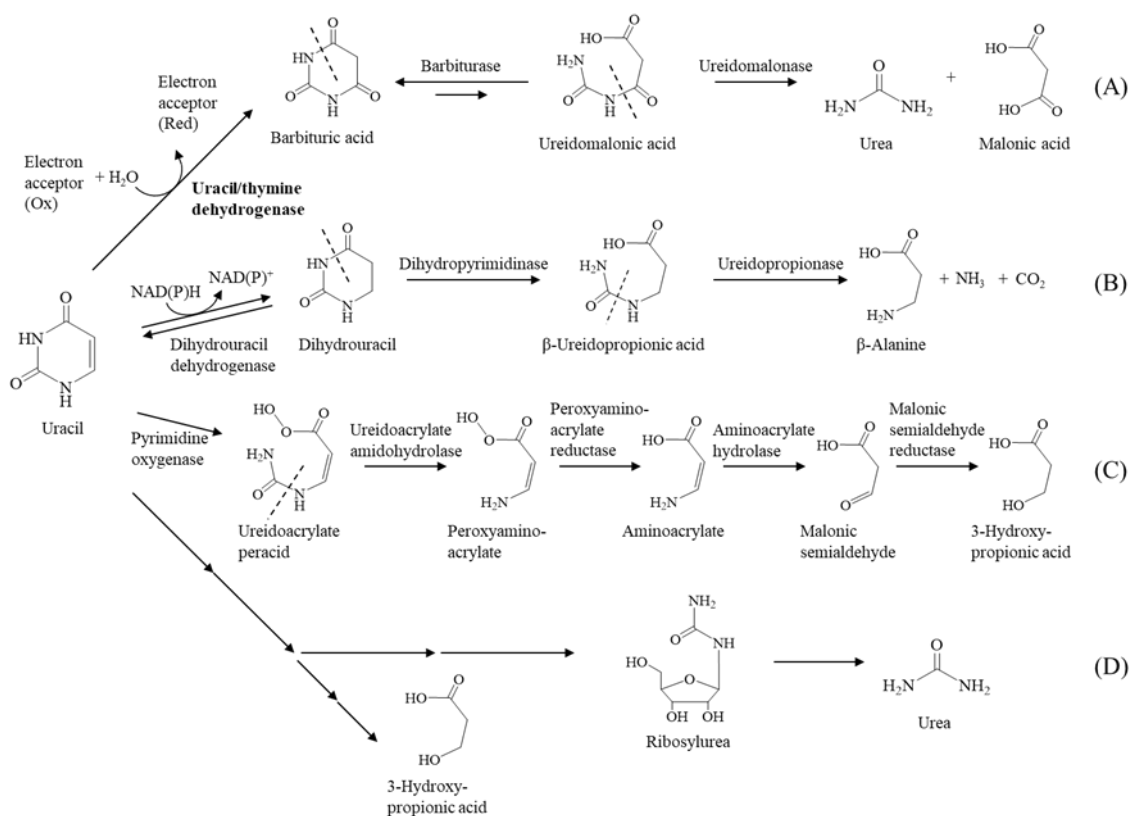


Fig. 3-1 Microbial metabolism of pyrimidine base

(A) Oxidative pathway (Hayaishi and Kornberg 1952; Lara 1952; Soong et al. 2001; Soong et al. 2002), (B) reductive pathway (Vogels and Drift 1976; Syltatk et al. 1999), (C) pyrimidine utilization (rut) pathway (Loh et al. 2006; Piskur et al. 2007; Osterman 2006), and (D) URC pathway (Rasmussen et al. 2014).

A); reductive pyrimidine pathway (Syltatk et al., 1999; Tsai & Axelrod, 1965; Vogels & Van der Drift, 1976), B); oxidative pyrimidine pathway (Hayaishi & Kornberg, 1952; Horinouchi, Soon, et al., 2012; Lara, 1952; Soong et al., 2001b, 2002; Wang & Lampen, 1952), C); pyrimidine utilization (rut) pathway (Loh et al., 2006; Osterman, 2006; Piškur et al., 2007).

Methods

Microorganisms and cultivation

Rhodococcus erythropolis JCM 3132, *Escherichia coli* DH5 α , and *E. coli* Rosetta2 (DE3) were used for the experiments on ureidomalonase. LB medium was used for cultivation of these strains. *R. erythropolis* was cultivated at 28 °C overnight with shaking. *E. coli* was cultivated at 37 °C overnight with shaking. When necessary, 50 μ g/mL ampicillin and 100 μ M IPTG were added to the media.

Gene cloning

Total genomic DNA of *R. erythropolis* JCM3132 was isolated using DNeasy Blood & Tissue Kit (QIAGEN, U.S.A.). For amplification of the gene sequence encoding for ureidomalonase, PCR amplification was performed with PrimeSTAR[®] GXL polymerase (TAKARA BIO INC., Japan), the forward primer (5'- gtttaactttaagaaggagatatacatatggttcgatgctgctgacctg -3') and the reverse primer (5'- gtttaactttaagaaggagatatacatatggttcgatgctgctgacctg -3') using the genomic DNA of *R. erythropolis* JCM3132 as template. ProFlex PCR System (Thermo Fisher Scientific, U.S.A.) was programmed for 30 cycles of denaturation at 98 °C for 10 seconds; annealing at 60 °C for 15 seconds; and extension at 68 °C for 90 seconds. The resulting 1.5-kb gene was purified by DNA extraction from the agarose gel utilizing Gel/PCR Extraction Kit (Nippon Genetics, Japan). The purified gene was ligated into pET21b (Merck KGaA, Germany), which was treated by NdeI and XhoI by utilizing In-Fusion HD Cloning Kit (TAKARA BIO INC., Japan), yielding plasmid pET21b-hisum. This was maintained in *E. coli* DH5 α , and the sequence of the inserted fragment was confirmed by Sanger sequencing using T7 forward and reverse primers.

Expression of ureidomalonase into *E. coli*

The gene encoding ureidomalonase with His-tag (C-terminus) was expressed in *E. coli* Rosetta2 cells. This strain was pre-cultured in 5 mL of LB medium containing 50 μ g/mL ampicillin at 37 °C overnight. 15 mL of pre-culture was inoculated into 750 mL of LB medium containing 50 μ g/mL ampicillin, and the main culture was incubated at 37 °C for 2 hours. After incubation, 75 μ L of 1 M IPTG was added, and the main culture was incubated at 16 °C overnight. The cells were harvested from 1.5 L of the main culture and then used for purification of ureidomalonase.

Purification of ureidomalonase

All purification steps were carried out at 0–5 °C. The buffer used was 20 mM potassium phosphate (pH 7.5) containing 5 mM imidazole, and 500 mM NaCl. Washed *E. coli* Rosetta2 cells overexpressing ureidomalonase with His-tag (6 g) were suspended in 12 mL of the buffer. The suspension was disrupted by ultrasonication utilizing INSONATOR 201M (KUBOTA, Japan) (200 W, 5 min/Total 20 minutes). The resulting supernatant was used as the cell-free extract. The cell-free

extracts were then applied to a His trap HP 5 mL pre-equilibrated with the buffer. The enzyme was eluted with a linear gradient of 5–100 mM imidazole in 1 L of the buffer, and the activity of the eluted fractions was measured using standard enzyme assay conditions (described below). The active fractions were combined and concentrated to less than 2 mL by ultrafiltration. 10 mL of 20 mM phosphate buffer (pH 7.5) was added to the concentrated solution and concentrated once again. 1 mL of glycerol was added to 1 mL of the concentrate and stored at $-20\text{ }^{\circ}\text{C}$.

Determination of ureidomalonase concentration

The concentration of ureidomalonase was determined by Bradford assay (Kielkopf et al., 2020). Bio-Rad Protein Assay Dye Reagent Concentrate (Bio-Rad Laboratories, Inc., U.S.A.) was utilized for the assay. 0.1, 0.05, 0.02, and 0.01 % (w/v) BSA were utilized as a standard protein for creating a calibration curve.

Enzyme assay

The standard assay mixture comprises 10 mM of ureidomalonic acid and 20 mM of KPB (pH 8.0) in 50 μL . The reactions were initiated by adding 5 μL of 2 ($\mu\text{g}/\text{mL}$) enzyme solutions at $30\text{ }^{\circ}\text{C}$ for 1 h and stopped with 5 μL of 15 % (v/v) perchloric acid. The reaction mixtures were then neutralized with 45 μL of 500 mM KPB (pH 8.0) and centrifuged at 15,000 rpm for 10 min. Urea production in the supernatants was analyzed. The enzymatic activity was defined as the amount of urea produced by HPLC analysis. 50 μL of supernatant was used for urea assay.

Substrate specificity of ureidomalonase was determined as follows: 10 mM of barbituric acid, β -ureidopropionic acid, and allantoin were tested in the same conditions as those of the standard assay mixture, but without the addition of partially purified barbiturase. These reaction mixtures were then subjected to HPLC analysis.

Stability of ureidomalonase

To determine the temperature stability of ureidomalonase, 50 μL of 2 ($\mu\text{g}/\text{mL}$) ureidomalonase was incubated at $10\text{--}70\text{ }^{\circ}\text{C}$ for 10 min, followed by cooling on ice. The resulting enzyme solutions were used for standard assay.

To determine the pH stability of ureidomalonase, 1 μL of 200 ($\mu\text{g}/\text{mL}$) ureidomalonase was added to 9 μL of each buffer (20 mM sodium citrate (pH2.5–3.5), sodium acetate (pH4.0–5.5), potassium phosphate (pH6.0–8.0), Tris/HCl (pH8.5, and 9.0), sodium carbonate (pH9.5–11), and sodium phosphate (pH11.5–12.5)), and incubated on ice for 10 min, followed by added to 90 μL of 20 mM potassium phosphate buffer (pH7.5). The resulting enzyme solutions were used for standard assay.

Urea assay

QuantiChrom Urea Assay Kit (BioAssay Systems, U. S. A.) was utilized for measuring urea concentration of the reaction mixture.

HPLC analysis

Urea, malonic acid, ureidomalonic acid, and reaction mixture of enzyme assay were analyzed by HPLC at 190 nm [column, YMC-Pack Polyamine II (4.6 × 250 mm, YMC CO., LTD., Japan); eluent, 50 mM NH₄H₂PO₄-H₃PO₄ (pH 2.8)/acetonitrile (20/80); flow rate, 1.0 mL/min; temperature, 37 °C].

SDS-PAGE

The purified ureidomalonase was analyzed through SDS-PAGE using a 12.5 % polyacrylamide gel, which was stained with Coomassie Brilliant Blue R-250. Protein concentrations were determined using the dye binding assay of Bradford (Bio-Rad Laboratories, Hercules, USA).

Induction of enzyme production in the gene cluster of the pyrimidine oxidative pathway

The medium, containing 2 g carbon source (uracil or glucose), 0.2 g yeast extract, 0.2 g tryptone, 1 g K₂HPO₄, 1 g KH₂PO₄, 0.5 g sea salt (Sigma-Aldrich, St. Louis, USA), 1 mg FeSO₄·7H₂O, 1 mg Na₂MoO₄·2H₂O, 1 mg MnSO₄, 1 mg CuSO₄, and 1 mg ZnCl₂ in 1 L of tap water, was used to induce the enzyme production in the gene cluster of the pyrimidine oxidative pathway. *R. erythropolis* JCM3132 was pre-cultured in 5 mL of this medium at 37 °C for 3 days. 3 pre-cultures (total: 15 mL) were inoculated into 750 mL of this medium, and the main culture was incubated at 37 °C for 3 days. The cells were harvested from 750 mL of the main culture. The cell free extract of *R. erythropolis* JCM3132 was obtained as described above except that the buffer was 100 mM Tris/HCl (pH 8.5).

Results

Purification, and substrate specificity of ureidomalonase

Purification: The purified fraction obtained with a His trap column described above gave a single protein band as visualized on SDS-PAGE (Fig. 3-2), corresponding to a theoretical molecular weight of 54,865. The concentration of purified enzyme solution mixed with the same volume of glycerol was 200 (µg/mL).

Substrate specificity: The purified ureidomalonase showed strict specificity towards ureidomalonic acid (Fig. 3-3-A). Indeed, a precursor of ureidomalonic acid (barbituric acid), the intermediate of pyrimidine reductive metabolism (β-ureidopropionic acid), and that of purine

metabolism (allantoin) were also tested as substrates. However, there were no peaks whose retention times perfectly match those of urea (Fig. 3-3-B-D). Moreover, the substrate other than ureidomalonic acid did not decrease after incubation (Fig. 3-4). It was indicated that ureidomalonase has strict catalytic activity against ureidomalonic acid.

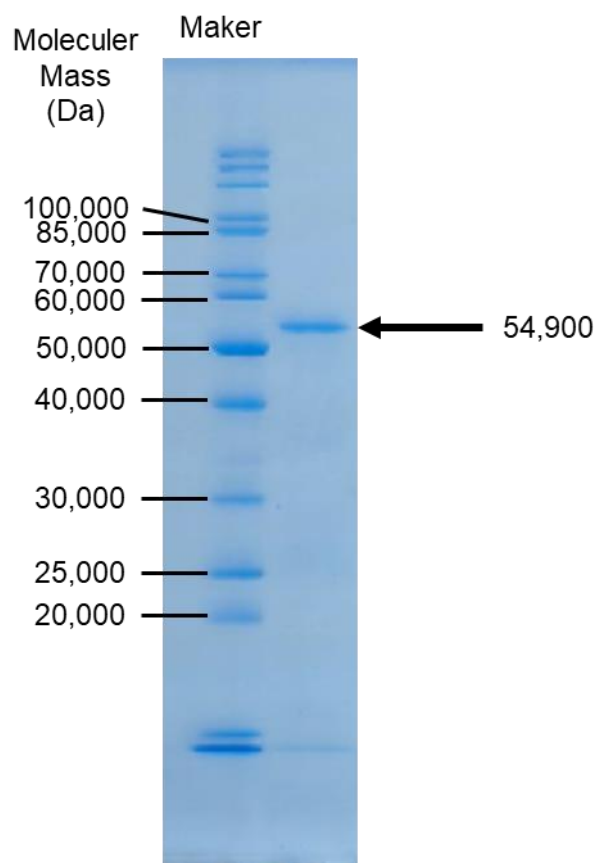


Fig. 3-2 Purified ureidomalonase on SDS-PAGE.

About 0.3 μg of ureidomalonase was applied to SDS-PAGE.

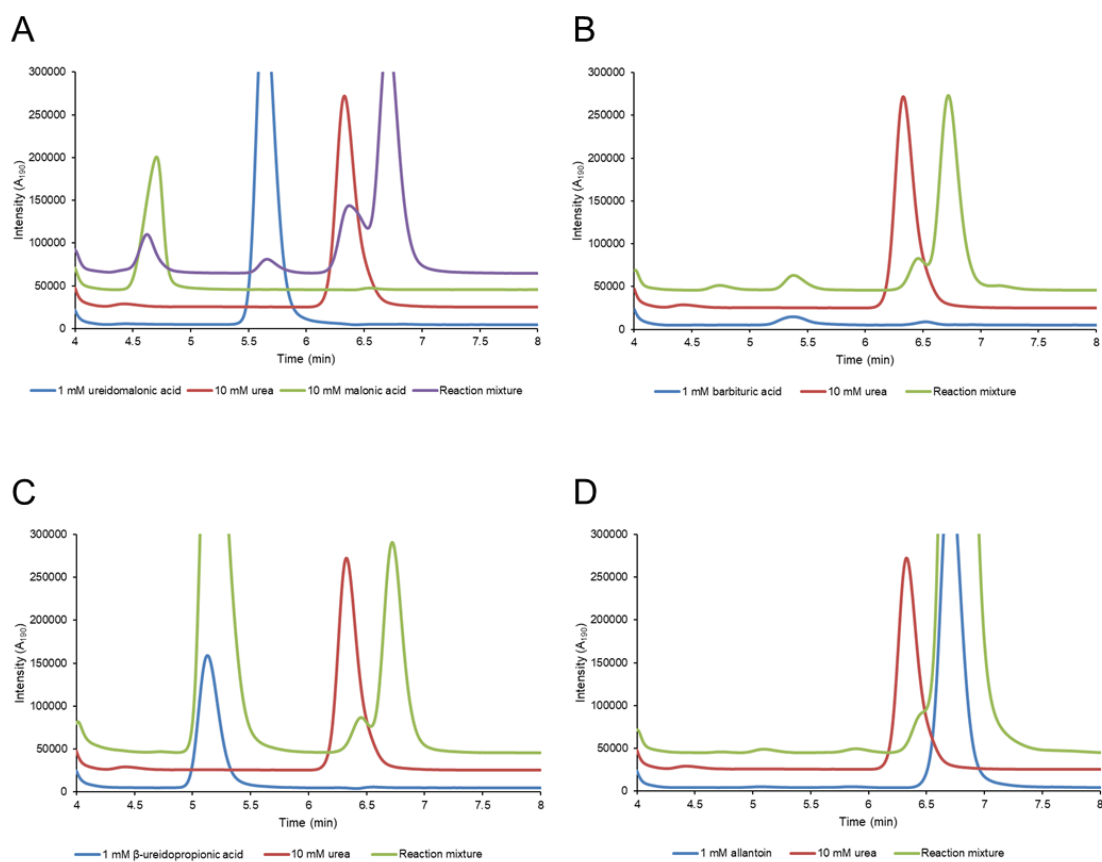


Fig. 3-3 HPLC analysis of reaction mixture of enzyme assay.

These figures show the results of HPLC analysis of a reaction mixture containing 10 mM ureidomalonic acid (A), barbituric acid (B), β -ureidopropionic acid (C), and allantoin (D).

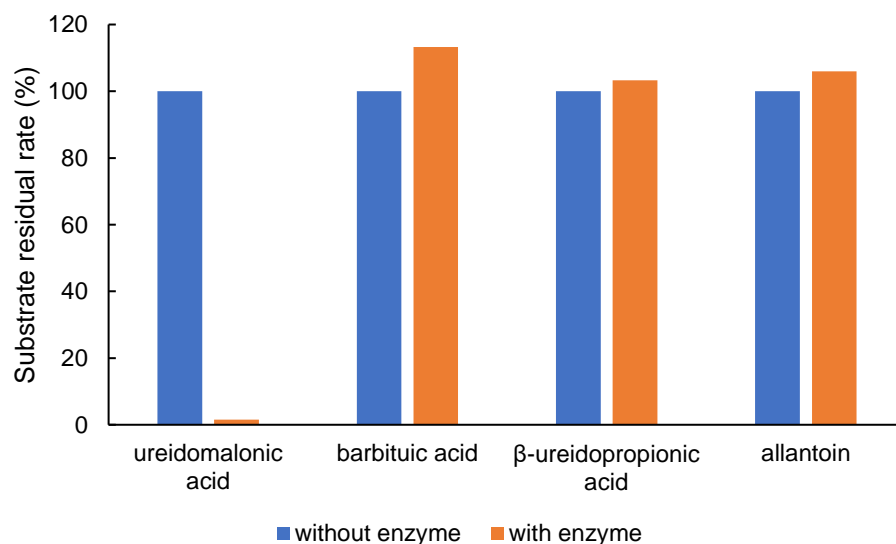


Fig. 3-4 Substrate residual rate after incubation.

The amount of the substrate after the incubation without the purified enzyme was defined as 100 %.

Effects of pH and temperature

Enzyme activity and stability were assayed in the buffer described above (20 mM) using purified enzyme. Under standard assay conditions, the highest activity was observed in Tris/HCl buffer, pH 8.5 (Fig.3-5-A). When the enzyme was incubated on ice for 10 min at pH 4–12.5, the activity was retained (Fig. 3-5-B). The hydrolysis reaction of ureidomalonic acid increased with temperature, reaching a maximum of 40 °C (Fig. 3-5-C). When the enzyme was incubated at 4–45 °C for 10 min, the activity was retained (Fig. 3-5-D).

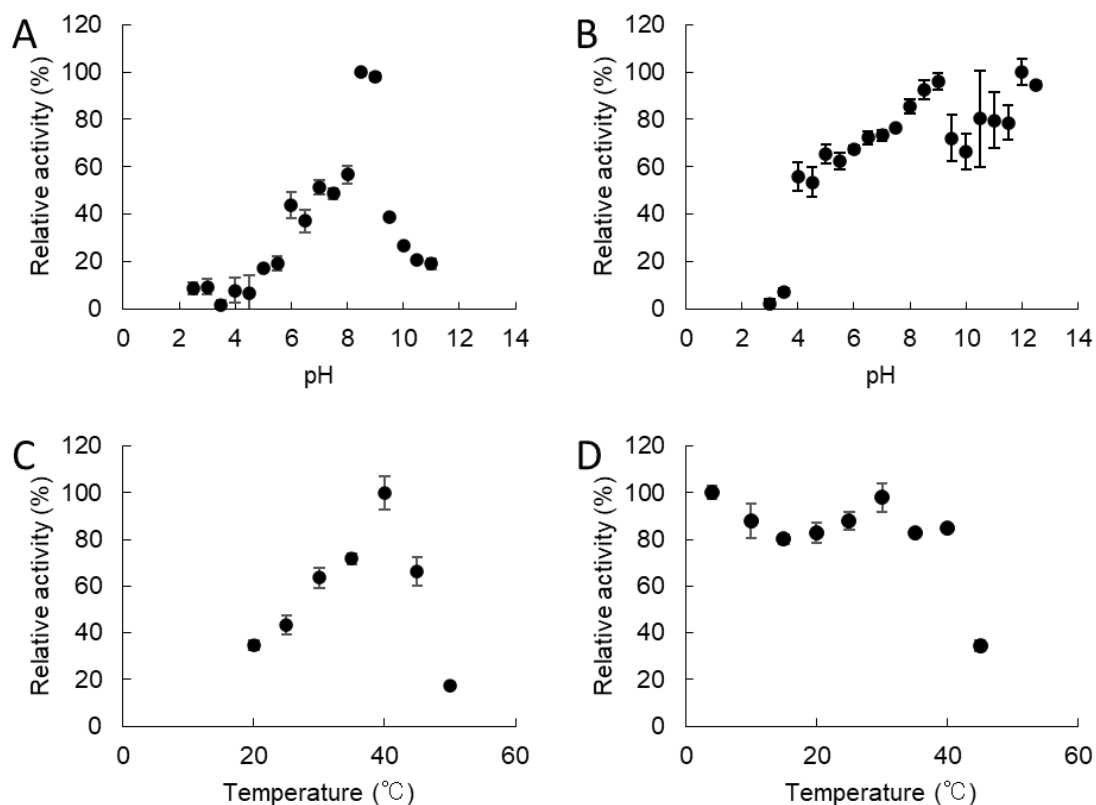


Fig. 3-5 Effect of reaction temperature and pH on activity and stability of ureidomalonase

A. Effect of pH. 20 mM sodium citrate (pH2.5–3.5), sodium acetate (pH4.0–5.5), potassium phosphate (pH6.0–8.0), Tris/HCl (pH8.5, and 9.0), and sodium carbonate (pH9.5–11) B. pH stability. 20 mM sodium citrate (pH2.5–3.5), sodium acetate (pH4.0–5.5), potassium phosphate (pH6.0–8.0), Tris/HCl (pH8.5, and 9.0), sodium carbonate (pH9.5–11), and sodium phosphate (pH11.5–12.5). C. Effect of reaction temperature. D. Thermal stability.

Homology analysis.

Amino acid sequence analysis determined that the purified protein showed homology with putative amidases described in *R. opacus* (NCBI; WP_005243547; 77 % identity), *Saccharopolyspora*

spinosa (NCBI; WP_010699428; 58 % homology), and *Pseudomonas* sp. M1 (NCBI; WP_009615078; 58 % homology), and glutamyl tRNA (Gln) amidotransferases such as that from *Lactobacillus plantarum* WCFS1 (Swiss-Prot; Q88XP7).

Characterization of pyrimidine oxidative pathway in *R. erythropolis*

Gene cluster of the pyrimidine oxidative pathway. The nucleotide sequence of an approximately 10-kb region around the ureidomalonase gene was determined using primers based on the strain PR4 gene. The ORFs of which functions have already been described are indicated in closed arrows (Fig. 3-6). Here, it is revealed that the 10-kb sequence contains 8 complete ORFs as determined by computer aided analysis and that the gene cluster of strain JCM3132 is almost the same (over 99 %) as that of strain PR4.

The enzyme production in the gene cluster of the pyrimidine oxidative pathway in *R. erythropolis* JCM3132 was induced by cultivation in the medium described above. The enzyme activity was determined with the addition of uracil or barbituric acid as a substrate in the enzymatic assay reaction. Results showed that the cells grown with uracil exhibited the enzymatic activities of UTDH, barbiturase, and ureidomalonase (Table 3-1). While barbituric acid was produced, malonic acid was not produced in the presence of uracil. On the other hand, cells grown in the presence of glucose as a carbon source exhibit no detectable levels of uracil or barbituric acid degradation. Altogether, these results indicate that expression of the enzymes encoded in the gene cluster is inducible by uracil.

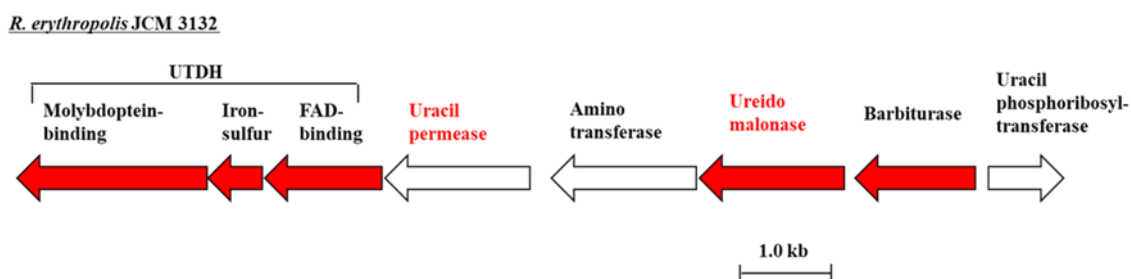


Fig. 3-6 Gene cluster of pyrimidine oxidative pathway in *R. erythropolis* JCM3132.

Closed arrows are ORFs, and their enzymatic functions were already revealed.

Table 3-1 Effect of uracil on the enzyme production involved in the gene cluster of the pyrimidine oxidative pathway.

culture	enzymatic reaction	substrates and products detection		
carbon source 0.1% each	substrate 5 mM each	in the enzymatic reaction (mM)		
		uracil	barbituric acid	malonic acid
uracil	* ¹ uracil	3.60	0.12	n.d.
uracil	* ² barbituric acid		n.d.	2.60
glucose	* ¹ uracil	5.00	n.d.	n.d.
glucose	* ² barbituric acid		5.00	n.d.
uracil + glucose	* ¹ uracil	3.24	0.07	n.d.
uracil + glucose	* ² barbituric acid		n.d.	2.50

*¹The reaction mixture contained, 100 mL of 5 mM uracil, 1 mM methylene blue (as electron acceptor), 100 mM Tris/HCl (pH 8.5), and an aliquot of cell-free extract of strain JCM3132. These reactions were performed at 30 °C for 1.5 h with shaking (160 rpm).

*²The reaction mixture contained 100 mL of 5 mM barbituric acid, 100 mM KPB (pH 8.5), and an aliquot of cell-free extract of strain JCM3132. These reactions were performed at 30 °C for 1.5 h with shaking (160 rpm).

n. d. indicates no detectable activity.

Discussion

To the best of our knowledge, this is the first study to describe the gene and protein function of ureidomalonnase in the oxidative degradation pathway of pyrimidine. Also, a clearer understanding of the structure and expression of the gene cluster associated with this pathway were provided. Ureidomalonnase did not show any catalytic activity towards linear amides (β -ureidopropionic acid, β -ureidoisobutyric acid), which represent intermediate products in the pyrimidine reductive pathway, nor towards allantoin and allantoic acid, which are intermediate products in purine metabolism. This enzyme showed resistance to high pH conditions. This feature is consistent with UTDH from *R. erythropolis* JCM3132. This enzyme did not exhibit any sequence similarity with β -ureidopropionase or carbomoylase, which represent its match in the reductive pathway and the hydantoin metabolism, respectively. Like ureidomalonnase, barbiturase did not exhibit any sequence similarity with dihydropyrimidinase or hydantoinase (Soong et al., 2002). This phenomenon suggests that the oxidative and reductive pathways of pyrimidine degradation have emerged from different evolutionary paths, as a result of environmental adaptation.

The gene cluster of the pyrimidine oxidative pathway was identified and the catalytic functions of UTDH (this study), barbiturase (Soong et al., 2002), and ureidomalonnase (this study) are

described. It is also revealed that the gene expression of this cluster is inducible in the presence of uracil (Table 3-1).

The function of one enzyme, which was annotated as a potential aminotransferase, remains unknown. Another putative uracil phosphoribosyltransferase is also adjoined to the gene cluster. Because this enzyme is involved in the salvage pathway for uracil in pyrimidine nucleosides synthesis, the collaboration of pyrimidine oxidative degradation and salvage synthesis, at both the catalytic and genetic level, may be suggested for regulation of pyrimidine pools in strains that degrade pyrimidine through the oxidative pathway. The final products of these latter pathways are malonic acid and urea. Malonic acid is commonly fused to CoA in living cells and serves as malonyl-CoA in fatty acid synthesis (Kim & Chae, 1991). On the other hand, it was reported that malonic acid plays a role as a precursor of oxaloacetate, which consists of its tricarboxylic acid cycle. In the case of *R. erythropolis*, malonic acid generated by ureidomalonnase might flow into fatty acid synthesis and energy production.

There is only one example of the successful application of pyrimidine oxidative metabolism in biotechnology, and this relates to controlling the equilibrium of ribose-transfer reaction between pyrimidine and purine. Pyrimidine nucleosides are easily synthesized by chemical methods, while purine nucleosides are not effectively synthesized due to the requirement for a complex multi-step process. In the enzymatic ribose-transfer reaction, thymidine is converted into 2'-deoxyguanosine via 2-deoxyribose 1-phosphate, a reaction catalyzed by pyrimidine nucleoside phosphorylase and purine nucleoside phosphorylase (Fig. 3-7) (Mikami et al. 2000). The critical but common issue in this process is fine control of the reaction equilibrium. In this case, the equilibrium between the substrate (pyrimidine nucleoside) and product (purine nucleoside) is inclined toward the substrate side and causes a low conversion yield of thymidine into 2'-deoxyguanosine (12 %). Thereupon, the addition of *Arthrobacter* sp. YGK22, which possesses a pyrimidine oxidative pathway into a base-exchange reaction led to the removal of free thymine from the reaction, and then the reaction equilibrium was shifted toward 2'-deoxyguanosine synthesis. As a result, the conversion yield was greatly increased (75 %) (Mikami et al. 2000). One of the notable advantages of the utilization of pyrimidine oxidative metabolism is that the reaction mixture does not necessarily need to be supplemented with expensive cofactors such as NAD(P). In the application context of the pyrimidine reductive pathway onto this ribose-transfer reaction, NAD(P)H might, however, be required because dihydrouracil dehydrogenase, which is an enzyme involved in the initial stages of the reductive pathway, requires it. In the case of *R. erythropolis* JCM3132 cells, the same positive effect as that of *Arthrobacter* sp. was observed (Mikami et al. 2000). Recently, in the field of nucleic acid medicine, the demand for nucleoside analogs is increasing as small interfering (si) RNA drugs and second-generation antisense drugs are tolerant to nuclease because of RNA interference mechanisms and chemical modifications of ribose. However, the chemical synthesis of purine nucleosides remains difficult. Therefore, it is hopeful that applying pyrimidine oxidative metabolism may contribute to increasing the productivity of purine

nucleosides and their analogs using the above ribose-transfer reactions. Along with the reductive and the rut pathways, knowledge of the oxidative pathway will provide some insight into the physiological importance of nucleic acid metabolism, and its potential contribution to biotechnology.

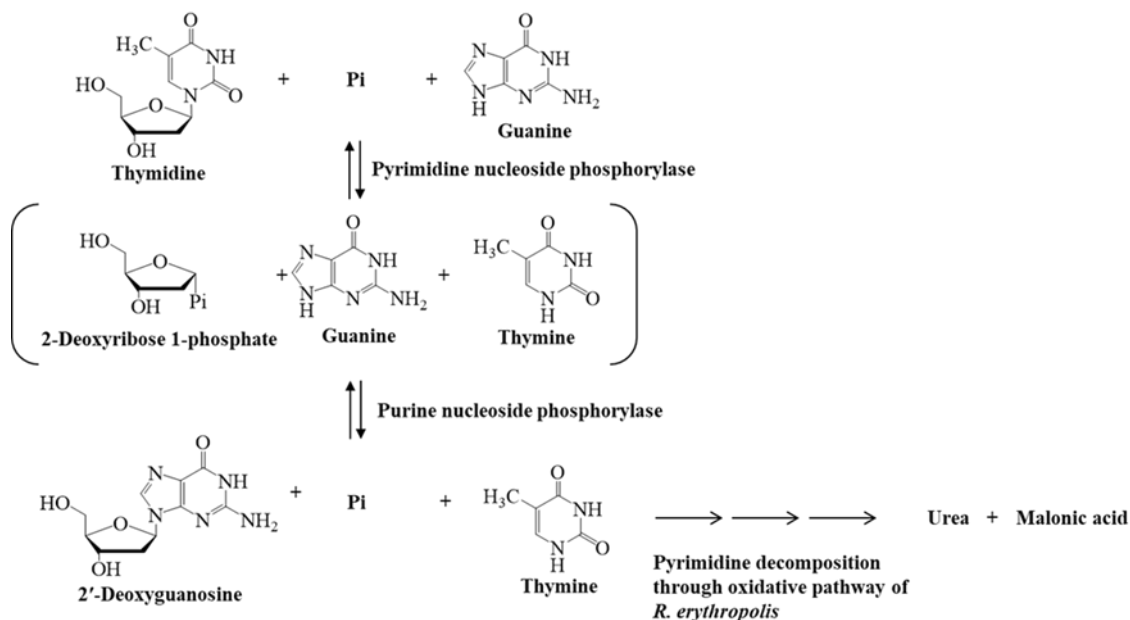


Fig. 3-7 Equilibrium control of ribose-transfer reaction between pyrimidine and purine by addition of pyrimidine oxidative degradation.

References

- Andersson Rasmussen, A., Kandasamy, D., Beck, H., Crosby, S. D., Björnberg, O., Schnackerz, K. D., & Piškur, J. (2014). Global Expression Analysis of the Yeast *Lachancea* (*Saccharomyces*) *kluuyveri* Reveals New *URC* Genes Involved in Pyrimidine Catabolism. *Eukaryotic Cell*, *13*(1), 31–42. <https://doi.org/10.1128/EC.00202-13>
- Hayaishi, O., & Kornberg, A. (1952). Metabolism of cytosine, thymine, uracil, and barbituric acid by bacterial enzymes. *The Journal of Biological Chemistry*, *197*(2), 717–732.
- Horinouchi, N., Soon, C.-L., Shimizu, S., & Ogawa, J. (2012). Oxidative pyrimidine metabolism in *Rhodococcus erythropolis* useful for valuable nucleoside synthesis: Discovery of a novel amidohydrolase, ureidomalonnase. *Biocatalysis and Agricultural Biotechnology*, *1*(3), 264–266. <https://doi.org/10.1016/j.bcab.2012.03.011>
- Kielkopf, C. L., Bauer, W., & Urbatsch, I. L. (2020). Bradford Assay for Determining Protein Concentration. *Cold Spring Harbor Protocols*, *2020*(4), 102269. <https://doi.org/10.1101/pdb.prot102269>
- Kim, Y. S., & Chae, H. Z. (1991). Purification and properties of malonyl-CoA synthetase from

- Rhizobium japonicum*. *Biochemical Journal*, 273(3), 511–516.
<https://doi.org/10.1042/bj2730511>
- Lara, F. J. S. (1952). ON THE DECOMPOSITION OF PYRIMIDINES BY BACTERIA II. *Journal of Bacteriology*, 64(2), 279–285. <https://doi.org/10.1128/jb.64.2.279-285.1952>
- Loh, K. D., Gyaneshwar, P., Markenscoff Papadimitriou, E., Fong, R., Kim, K.-S., Parales, R., Zhou, Z., Inwood, W., & Kustu, S. (2006). A previously undescribed pathway for pyrimidine catabolism. *Proceedings of the National Academy of Sciences*, 103(13), 5114–5119. <https://doi.org/10.1073/pnas.0600521103>
- Osterman, A. (2006). A hidden metabolic pathway exposed. *Proceedings of the National Academy of Sciences*, 103(15), 5637–5638. <https://doi.org/10.1073/pnas.0601119103>
- Parales, R. E., & Ingraham, J. L. (2010). The Surprising Rut Pathway: an Unexpected Way To Derive Nitrogen from Pyrimidines. *Journal of Bacteriology*, 192(16), 4086–4088. <https://doi.org/10.1128/JB.00573-10>
- Piškur, J., Schnackerz, K. D., Andersen, G., & Björnberg, O. (2007). Comparative genomics reveals novel biochemical pathways. *Trends in Genetics*, 23(8), 369–372. <https://doi.org/10.1016/j.tig.2007.05.007>
- Soong, C.-L., Ogawa, J., Sakuradani, E., & Shimizu, S. (2002). Barbiturase, a Novel Zinc-containing Amidohydrolase Involved in Oxidative Pyrimidine Metabolism. *Journal of Biological Chemistry*, 277(9), 7051–7058. <https://doi.org/10.1074/jbc.M110784200>
- Soong, C.-L., Ogawa, J., & Shimizu, S. (2001a). Cyclic ureide and imide metabolism in microorganisms producing a d-hydantoinase useful for d-amino acid production. *Journal of Molecular Catalysis B: Enzymatic*, 12(1–6), 61–70. [https://doi.org/10.1016/S1381-1177\(00\)00204-6](https://doi.org/10.1016/S1381-1177(00)00204-6)
- Soong, C.-L., Ogawa, J., & Shimizu, S. (2001b). Novel Amidohydrolytic Reactions in Oxidative Pyrimidine Metabolism: Analysis of the Barbiturase Reaction and Discovery of a Novel Enzyme, Ureidomalonase. *Biochemical and Biophysical Research Communications*, 286(1), 222–226. <https://doi.org/10.1006/bbrc.2001.5356>
- Syldatk, C., May, O., Altenbuchner, J., Mattes, R., & Siemann, M. (1999). Microbial hydantoinases - industrial enzymes from the origin of life? *Applied Microbiology and Biotechnology*, 51(3), 293–309. <https://doi.org/10.1007/s002530051395>
- Tsai, C. S., & Axelrod, B. (1965). Catabolism of Pyrimidines in Rape Seedlings. *Plant Physiology*, 40(1), 39–44. <https://doi.org/10.1104/pp.40.1.39>
- Vogels, G. D., & Van der Drift, C. (1976). Degradation of purines and pyrimidines by microorganisms. *Bacteriological Reviews*, 40(2), 403–468. <https://doi.org/10.1128/br.40.2.403-468.1976>
- Wang, T. P., & Lampen, J. O. (1952). Metabolism of pyrimidines by a soil bacterium. *The Journal of Biological Chemistry*, 194(2), 775–783.

Conclusion

Currently, the only known biosynthesis of deoxyribonucleotides in living organisms is the reduction reaction of ribonucleotides by ribonucleotide reductase (RNR) (RNR pathway). On the other hand, it was confirmed that deoxyribonucleosides can be synthesized by utilizing the enzyme function of the 2-deoxyribose-5-phosphate aldolase (DERA) pathway, which is a deoxyribonucleoside degradation pathway. This suggests that DNA constituent molecules can be biosynthesized by routes other than the RNA pathway and casts doubt on the RNA origin theory for the origin of living molecules. The study in Chapter 1 provides valuable insight into the possibility of alternative RNR pathways by other DNA component synthesis systems.

There are four alternative pathways for pyrimidine degradation in biological systems: the oxidative pathway, the reductive pathway, the pyrimidine utilization (rut) pathway, and the URC pathway. In the oxidative pathway, pyrimidine is degraded to urea and malonic acid via a barbituric acid derivative. The oxidative pathway of pyrimidine metabolism was first reported in *Mycobacterium*, *Corynebacterium*, and *Nocardia* strains isolated from soil. However, the precise understanding of oxidative pyrimidine metabolism was not established. The studies in Chapter 2 provide novel information on enzymes in oxidative pyrimidine metabolism.

In Chapter 1, the RNR knockout strain of *Escherichia coli* BW38029 was constructed (Δ RNR). This strain required only deoxycytidine among deoxyribonucleosides (dNSs) for growth. Supply of deoxycytidine (dC) through the DERA pathway has not been confirmed, and so far, replacement of the RNR pathway with the DERA pathway has not been achieved, but this may be resolved by coupling nucleoside-deoxyribosyltransferase II (ndtII) to the DERA pathway. Interestingly, the growth of this strain was enhanced by vitamins, especially nicotinamide, which was essential for growth. It was suggested that knockout of RNR may affect not only dNS synthesis but also other metabolic pathways. From these results, its complete synthetic medium was proposed, which is the MOPS medium containing dC and nicotinamide.

In Section 1 of Chapter 2, uracil-thymine dehydrogenase (UTDH), which catalyzes the irreversible oxidation of uracil to barbituric acid in oxidative pyrimidine metabolism, was purified from *Rhodococcus erythropolis* JCM 3132. The finding of unusual stabilizing conditions (high alkaline, pH 11, in the presence of NADP⁺ or NADPH) enabled the enzyme purification. The purified enzyme was found to be a heteromer consisting of three different subunits. The enzyme catalyzed oxidation of uracil to barbituric acid with artificial electron acceptors such as methylene blue, phenazine methosulfate, benzoquinone, and α -naphthoquinone; however, NAD⁺, NADP⁺, flavin adenine dinucleotide, and flavin mononucleotide did not serve as electron acceptors. The enzyme acted not only on uracil and thymine but also on 5-halogen-substituted uracil and hydroxypyrimidine (pyrimidone), while dihydropyrimidine, which is an intermediate in reductive pyrimidine metabolism,

and purine did not serve as substrates. Interestingly, the activity of UTDH was enhanced by cerium ions, and this activation was observed with all combinations of substrates (uracil, thymine, 5-fluorouracil) and electron acceptors (methylene blue, phenazine methosulfate, benzoquinone, α -naphthoquinone).

In Section 2 of Chapter 2, ureidomalonnase from *R. erythropolis* JCM3132 was purified to homogeneity as a functional protein from *E. coli* Rosetta2 (DE3) overexpressing this enzyme, and it was shown that this purified enzyme catalyzes the amidohydrolysis of ureidomalonic acid into urea and malonic acid. It was also shown that the enzyme exhibited a strict specificity toward ureidomalonic acid. Importantly, gene expression of the gene cluster of the pyrimidine oxidative degradation pathway was shown to be inducible by addition of uracil. An example of the utilization of pyrimidine oxidative metabolism is described in the context of biotechnology. Indeed, it was demonstrated that the pyrimidine oxidative degradation could be useful in the equilibrium control of ribose transfer between pyrimidine and purine bases, with a significant increase in the conversion yield of purine nucleoside synthesis.

Altogether, this research suggests that other pathways may replace the RNR pathway. Δ RNR required dC for growth. Although synthesis of dC via the DERA pathway could not be confirmed, other dNSs can be synthesized, indicating the possibility of synthesizing dC by conjugation with NdtII. This research also provides detailed information on enzymes involved in oxidative pyrimidine metabolism. UTDH catalyzes the irreversible oxidation of uracil to barbituric acid in oxidative pyrimidine metabolism. The enzyme was revealed to be composed of three different subunits, each containing an FAD-binding site, an iron-sulfur cluster, and a molybdenum-binding site. Ureidomalonnase catalyzes the amidohydrolysis of ureidomalonic acid into urea and malonic acid. It was also shown that the enzyme exhibited a strict specificity toward ureidomalonic acid.

Acknowledgements

The author wishes to express my deepest gratitude to Professor Jun Ogawa for his thoughtful guidance, warm encouragement, and kind supports during the course of this study.

The author greatly appreciates Assistant Professor Michiki Takeuchi for his continuous guidance and constructive suggestions. Without his persistent support, this thesis would not have been possible.

The author also wishes to thank Professor Anthony M Poole, University of Auckland, for his helpful suggestions and technical supports.

The author gratefully acknowledges Professor Makoto Ueda, Professor Tomohiro Fujita, Associate Professor Ryota Hara, Associate Professor Shigenobu Kishino, Assistant Professor Akinori Ando, Assistant Professor Ryota Kikuchi, an Assistant Professor Hiroko Watanabe for their informative advice and kind suggestions throughout this work.

The author greatly appreciates Ms. Atsuko Kitamura and all members of the Laboratory of Fermentation Physiology and Applied Microbiology, Division of Applied Life Sciences, Graduate School of Agriculture, Kyoto University.

Finally, the author sincerely thanks my family and my friends.

Publications

1. Kengo Deguchi, Nobuyuki Horinouchi, Syoko Kozono, Michiki Takeuchi, Dayoung Si, Makoto Hibi, Anthony M. Poole, Jun Ogawa: The design of complete synthetic medium for ribonucleotide reductase disrupted strain of *Escherichia coli* BW38029. In preparation.
2. Chee-Leong Soong, Kengo Deguchi, Michiki Takeuchi, Nobuyuki Horinouchi, Dayong Si, Makoto Hibi, Sakayu Shimizu, and Jun Ogawa: Characterization of the initial enzyme in pyrimidine oxidative metabolism, uracil-thymine dehydrogenase. In preparation.
3. Kengo Deguchi, Michiki Takeuchi, Chee-Leong Soong, Nobuyuki Horinouchi, Sakayu Shimizu, Jun Ogawa: Heterologous expression and characterization of ureidomalonase. In preparation.
4. Samantha D M Arras, Nellie Sibaeva, Ryan J Catchpole, Nobuyuki Horinouchi, Dayong Si, Alannah M Rickerby, Kengo Deguchi, Makoto Hibi, Koichi Tanaka, Michiki Takeuchi, Jun Ogawa, Anthony M Poole: Characterisation of an *Escherichia coli* line that completely lacks ribonucleotide reduction yields insights into the evolution of parasitism and endosymbiosis. *Elife*.
2023 Apr 6